Journal of Sound and Vibration (1998) **213**(2), 259–299

VIBRATIONS OF PARTIALLY FILLED CYLINDRICAL TANKS WITH RING-STIFFENERS AND FLEXIBLE BOTTOM

M. Amabili

Department of Industrial Engineering, *University of Parma*, *Viale delle Scienze*, 43100 *Parma*, *Italy*

M. P. Païdoussis

Department of Mechanical Engineering, *McGill University*, 817 *Sherbrooke Street W.*, *Montreal*, *Québec*, *Canada H3A 2K6*

AND

A. A. Lakis

Department of Mechanical Engineering, *École Polytechnique*, *Montreal*, *Québec*, *Canada H3C 3A7*

(*Received* 20 *May* 1997, *and in final form* 22 *December* 1997)

The dynamics of a tank partially filled with a liquid having a free surface is investigated. In the analysis, the effect of free surface waves is taken into account, so that both bulging and sloshing modes are studied. The structure is completely flexible, and is composed of a vertically standing circular cylindrical shell, with ring-stiffeners, and a flexible bottom that consists of a circular plate generally resting on an elastic Winkler foundation. The plate edge is joined to the shell by coupling rotational springs distributed around the edge. The interaction between the plate and the shell via the fluid is included. Application to the particular cases of (i) a flexible shell with a rigid bottom and (ii) a flexible bottom plate with a rigid cylinder are also presented, as well as a comparison with approximate theories. Ring-stiffeners on the shell are also considered in order to investigate their influence on the modal behaviour of the tank. Solution of this problem is achieved via the method of artificial springs within the framework of the Rayleigh–Ritz theory, while considering strong fluid–structure interaction.

1. INTRODUCTION

The safety of tanks is a problem that has interested many investigators in the past, and still does so. Such tanks are used in many branches of engineering to store fluids. Most frequently, these tanks are vertical, cylindrical, of circular cross-section, and they are usually partially filled with liquids having a free surface. Most of the studies in the past dealt with partially filled tanks consisting of either (a) a rigid tank with a flexible bottom [1–7], or (b) a flexible shell with a rigid bottom [2, 8–14]. Many other studies deal with circular cylindrical shells or circular plates in particular configurations; see, e.g., references [15–31]. Bauer and Siekmann [32] studied a circular cylindrical flexible shell with a flexible bottom; however, they considered the plate and shell not joined together, while in reality they are. In contrast, Amabili [33] studied a tank partially filled with liquid composed of a circular cylindrical shell and a circular bottom plate resting on an elastic foundation, coupled together at the bottom edge by an elastic or rigid joint. The solution was reached

0022–460X/98/220259 + 42 $25.00/0/sv971481

by using artificial springs in the Rayleigh–Ritz method. This method was also successfully applied by other researchers in the last few years to the study of systems that can be modelled with simple components joined together [34–40]. However, in Amabili's paper [33], only bulging modes (where the tank wall oscillates, moving the liquid) are studied, and consequently the effect of free surface waves of the liquid is neglected; in particular a zero dynamic pressure on the free surface of the liquid was imposed.

Al-Najafi and Warburton [41] studied an empty ring-stiffened circular cylindrical shell. Harari *et al*. [42] studied a stiffened and submerged cylindrical shell closed by two end plates, but in this case the fluid around the shell was infinite, so that there was no free surface. Moreover, in contrast to Amabili [33], they neglected the interaction between the plates and the shell via the fluid and used the expression for the fluid load on the end plates obtained for circular plates with a rigid extension (circular plate in an infinite baffle).

The tank investigated in the present study is partially filled with a liquid having a free surface, and the effect of the free surface waves is taken into account, so that both bulging and sloshing (where the amplitude of the free surface waves is larger than the wall displacement) modes are studied. In fact, the free surface motion and oscillations of the tank walls can be significantly coupled for some geometries; consequently, a study such as this becomes important in some applications, e.g., propellent tanks of liquid-propellant rockets, where very flexible structures are employed. The tank considered here is completely flexible and composed of a vertical circular cylindrical shell with ring-stiffeners; it has a flexible bottom, consisting of a circular plate that can be considered to rest on an elastic Winkler foundation. The plate is joined to the shell, so that the relative rotation at the joint is zero (see Figure 1); however, the effect of elasticity of the joint is also investigated. The interaction between the plate and the shell via the fluid is included in the present study, as well as the effect of the in-plane load on the bottom plate, e.g., due to the weight of the liquid inside. Both the shell and the plate are made of linearly elastic material and have uniform thickness, so that the classical linear theory of elasticity of plates and shells may be utilized.

The present method is applied also to the particular cases of a flexible shell with a rigid bottom (section 6.1) and of a rigid cylinder with a flexible bottom plate (section 6.2), in order to compare the present computations with the experimental and theoretical data available in the literature and to give additional results. Comparison of sloshing modes in a flexible and a rigid tank is performed (section 6.3), as well as comparison of bulging modes retaining or neglecting the effect of free surface waves (section 6.3). A discussion of the accuracy of the simplified models is given. The influence of ring-stiffeners in the modal characteristics of the vibration of the tank is also discussed (section 6.4). The method used to obtain the solution is that of artificial springs in the Rayleigh–Ritz method, in the case of strong fluid–structure interaction, as developed in reference [43].

2. THE EMPTY TANK

In a tank section containing the tank axis, the rotation at the plate edge is considered joined to the rotation at the bottom edge of the shell, as discussed in references [33, 44]. Only this connection is required to study accurately lower modes of the system. The shell and the plate are connected together by artificial rotational springs of appropriate stiffness, continuously distributed around the circumference; the geometry of the system is shown in Figure 1.

The joint between the plate and the shell gives a reciprocal constraint that can be assumed to be a simple support for both the shell and the plate, the reciprocal rotation being coupled as previously discussed. Usually, storage tanks are covered by a roof

consisting of a top plate, sometimes supported by steel trusses. This roof is introduced in order to guarantee that the top section of the shell remains circular and undeformed, under the action of both static and dynamic loads, and of course to separate the internal liquid from the exterior. In fact, this constraint gives a significant increase to the tank stiffness. The effect of the roof can be simulated by a simple support at the top end of the shell for all the modes of vibration without movement of the tank axis. On the other hand, for beam-bending modes of storage tanks the cross-section of the shell remains circular but it moves with respect to the base, so that the top plate does not constrain these modes; hence, these modes may be studied correctly by considering a free top end of the shell. In the present study, the shell is considered to be simply supported at both ends, so that this model cannot be used to study the beam-bending modes. The top plate is included in the study only as a constraint. In fact, it is not coupled to the liquid inside the tank, and its modes are largely uncoupled with respect to the whole system, so that they are not very interesting for the present study. However, they could be retained without complicating significantly the present theory. Similar considerations can be made for propellant tanks.

The joint between the ring-stiffener and the shell involves the connections of the reciprocal transverse displacement and the reciprocal rotation in the plane of the cross-section, with neglect of the connections in the tangential plane. However, flexural modes of the ring are usually more important than torsional modes, so that in the present study only the reciprocal transverse displacement of the shell and ring are considered coupled, by introducing a distributed translational spring acting in the radial direction at the joint cross-section. This spring is also continuously distributed along a circle. The stiffness of this spring is chosen to be very high with respect to the stiffness of the flexible components of the tank, in order to simulate a welded connection between the shell and the ring. Thus, the effect of the rotation of the ring-stiffener in the plane of the cross-section is neglected.

The circular cylindrical tank considered has radius a, height L and is conveniently studied in the polar co-ordinates (r, θ, x); the origin of the co-ordinate system is placed at the centre of the bottom plate on the mean plane. Due to the axial symmetry of the structure, only modes of the shell and the plate with the same number n of nodal diameters are coupled. A nodal diameter is a diameter in the cross-section of the shell (or in the plane of the plate) connecting points which are immobile during vibration. Besides, it is

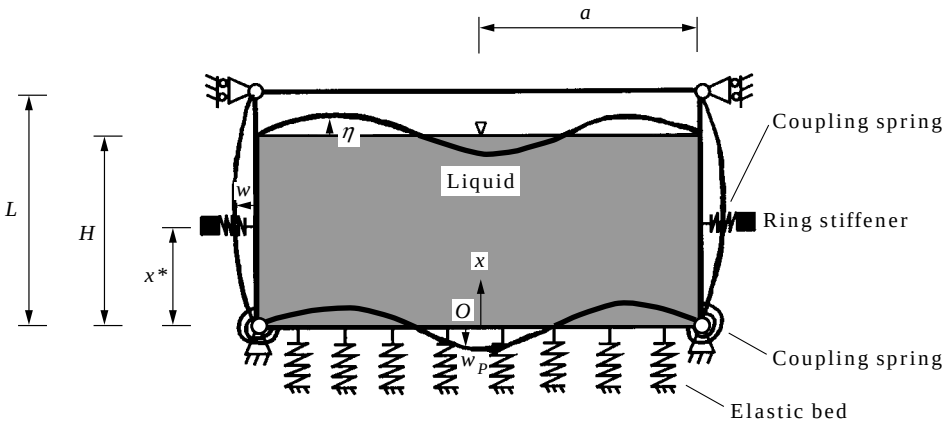

Figure 1. Geometry of the tank and co-ordinate system.

interesting to note that, due to axial symmetry, for each asymmetric mode ($n > 0$) there exists a second mode having the same frequency and shape but angularly rotated by $\pi/2n$.

The Rayleigh–Ritz method [43, 45] is applied to find natural modes of the tank, the time variation being assumed to be harmonic. Therefore, the mode shapes w of the shell wall in the radial direction (see Figure 1) can be expressed as

$$w(x, \theta) = \cos(n\theta) \sum_{s=1}^{\infty} q_s B_s \sin(s\pi x/L), \tag{1}$$

where n and s are the number of nodal diameters and of axial half-waves, q_s are the parameters of the Ritz expansion, and B_s is a constant depending on the normalization criterion used. The eigenvectors of the empty simply supported cylindrical shell (also called the shear diaphragm [46]) are used as admissible functions. Then the following normalization is introduced,

$$(L/a)^2 \int_0^1 B_s^2 \sin^2(s\pi l)\, \mathrm{d}l = 1, \tag{2}$$

where $l = x/L$. The integration gives

$$B_s = B = \sqrt{2}a/L. \tag{3}$$

The mode shapes w_P of the bottom circular plate in the transverse direction of the plate can be given as [47]

$$w_P(r, \theta) = \cos(n\theta) \sum_{i=0}^{\infty} \tilde{q}_i [A_{ni} \mathrm{J}_n(\lambda_{ni} r/a) + C_{ni} \mathrm{I}_n(\lambda_{ni} r/a)], \tag{4}$$

where n and i are the number of nodal diameters and circles, respectively, a is the plate radius, $\tilde{q}_i$ are the parameters of the Ritz expansion, and λ_{ni} is the well-known frequency parameter that is related to the plate natural frequency; J_n and I_n are the Bessel function and modified Bessel function of order n, respectively. In equation (4), the *in vacuo* eigenfunctions of the simply supported circular plate are assumed as admissible functions. The trial functions are linearly independent and constitute a complete set. Values of λ_{ni} for simply supported plates are given, for example, in reference [48]. To simplify the computations, the mode shape constants, A_{ni} and C_{ni}, are normalized in order to have (see equations 11.106, 33.101 and 31.101 in reference [49])

$$\int_0^1 [A_{ni} \mathrm{J}_n(\lambda_{ni}\rho) + C_{ni} \mathrm{I}_n(\lambda_{ni}\rho)]^2 \rho\, \mathrm{d}\rho$$

$$= \left\{ \frac{A_{ni}^2}{2} \left[(\mathrm{J}_n'(\lambda_{ni}))^2 + \left(1 - \frac{n^2}{\lambda_{ni}^2}\right) \mathrm{J}_n^2(\lambda_{ni}) \right] - \frac{C_{ni}^2}{2} \left[(\mathrm{I}_n'(\lambda_{ni}))^2 - \left(1 + \frac{n^2}{\lambda_{ni}^2}\right) \mathrm{I}_n^2(\lambda_{ni}) \right] \right.$$

$$\left. + \frac{A_{ni} C_{ni}}{\lambda_{ni}} [\mathrm{J}_n(\lambda_{ni}) \mathrm{I}_{n+1}(\lambda_{ni}) + \mathrm{I}_n(\lambda_{ni}) \mathrm{J}_{n+1}(\lambda_{ni})] \right\} = 1, \tag{5}$$

where $\rho = r/a$ and J_n' and I_n' indicate the derivatives of J_n and I_n with respect to the argument. The ratio of the mode shape constants for simply supported plates is

$$A_{ni}/C_{ni} = -I_n(\lambda_{ni})/J_n(\lambda_{ni}). \tag{6}$$

In order to solve the problem, the kinetic and potential energies of the shell, plate, ring-stiffeners, liquid, elastic foundation and coupling springs are evaluated. The reference kinetic energy T_S^* [45] of the shell, neglecting the tangential and rotary inertia, is given by

$$T_S^* = \frac{1}{2}\rho_S h_S B^2 \int_0^{2\pi}\int_0^L w^2 \,\mathrm{d}x\, a\,\mathrm{d}\theta = \frac{1}{2}\rho_S a\, h_S \frac{L}{2} B^2 \psi_n \sum_{s=1}^{\infty} q_s^2, \tag{7}$$

where h_S is the shell thickness, ρ_S is the density of the shell material (kg/m^3) and $\psi_n = \{2\pi \text{ for } n = 0,\ \pi \text{ for } n > 0\}$. In equation (7) the orthogonality of the sine function has been used. Similarly, the reference kinetic energy T_P^* of the plate is given by

$$T_P^* = \frac{1}{2}\rho_P h_P \int_0^{2\pi}\int_0^a w_P^2\, r\,\mathrm{d}r\,\mathrm{d}\theta = \frac{1}{2}\rho_P a^2 h_P \psi_n \sum_{i=0}^{\infty} \tilde{q}_i^2, \tag{8}$$

where h_P is the plate thickness and ρ_P is the density of the plate material (kg/m^3). In equation (8) the orthogonality of Bessel functions (plate mode shapes) has been used.

The flexural modes w_R of a ring-stiffener of the circular shell are [50]

$$w_R(\theta) = G_n \cos(n\theta), \tag{9}$$

and the reference kinetic energy of this element, upon neglecting the tangential inertia and considering only the rotary inertia due to the flexural displacement, is [41]

$$T_R^* = \frac{1}{2}\rho_R h_R L_R \int_0^{2\pi} [w_R^2 + (\partial w_R/\partial\theta)^2/a^2] a\,\mathrm{d}\theta = \frac{1}{2}\rho_R h_R L_R a\,\psi_n G_n^2 (1 + K_x n^2/a^2), \tag{10}$$

where h_R is the ring thickness, L_R is the ring width, ρ_R is the density of the ring material, K_x is the second moment of area of the ring cross-section about the axis parallel to x and through the centre of area of the cross-section, and G_n is the amplitude coefficient; obviously, the width L_R of the ring should be small.

Now it is useful to note that the maximum potential energy of each mode of the empty shell (without the bottom plate) is equal to the reference kinetic energy of the same mode multiplied by the circular frequency squared, ω_s^2, of this mode. Moreover, due to the series expansion of the mode shape, the potential energy is the sum of the energies of each single component mode. As a consequence, the maximum potential energy of the shell may be expressed as

$$V_S = \frac{1}{2}\rho_S h_S a \frac{L}{2} B^2 \psi_n \sum_{s=1}^{\infty} q_s^2 \omega_s^2, \tag{11}$$

where ω_s are the circular frequencies of the flexural modes of the simply supported shell that can be computed by using, for example, the Flügge theory of shells [46]. Similarly, the maximum potential energy of the plate is the sum of the reference kinetic energies of the eigenfunctions of the plate in vacuum multiplied by $\tilde{\omega}_{ni}^2$, i.e.,

$$V_P = \frac{1}{2}\rho_P a^2 h_P \psi_n \sum_{i=0}^{\infty} q_i^2 \tilde{\omega}_{ni}^2 = \frac{1}{2}\frac{D}{a^2}\psi_n \sum_{i=0}^{\infty} \tilde{q}_i^2 \lambda_{ni}^4, \tag{12}$$

where the plate circular frequency $\tilde{\omega}_{ni}$ is related to the frequency parameter λ_{ni} by $\tilde{\omega}_{ni} = (\lambda_{ni}^2/a^2)[D/(\rho_P h_P)]^{1/2}$ and $D = E_P h_P^3/[12(1-\nu_P^2)]$ is the flexural rigidity of the plate; ν_P and E_P are the Poisson's ratio and Young's modulus of the plate, respectively. Now, the maximum potential energy of a ring stiffener associated with transverse vibrations is

$$V_R = \frac{1}{2}\rho_R h_R L_R a\, \psi_n \omega_{R_n}^2 G_n^2 (1 + K_x n^2/a^2), \tag{13}$$

where ω_{R_n} is the natural circular frequency of transverse vibration of the ring alone for each n. This frequency can be computed by the classical bi-quadratic equation that is reported, for example, in reference [50].

The maximum potential energy of the distributed rotational springs connecting the plate and the shell is

$$V_{C_{P-S}} = \frac{1}{2}\int_0^{2\pi} c_1 \left[\left(\frac{\partial w}{\partial x}\right)_{x=0} - \left(\frac{\partial w_P}{\partial r}\right)_{r=a}\right]^2 a\, \mathrm{d}\theta, \tag{14}$$

where c_1 is the spring stiffness (Nm/m). It should be noted that the sign of rotations is attributed by considering that both w and w_P are positive outside the tank (see Figure 1), so that both displacements give a positive contribution to the increment of the angle between the shell and the plate, which gives a compression to the rotational spring. The rotation of the shell end at $x = 0$ is given by

$$\left(\frac{\partial w}{\partial x}\right)_{x=0} = \frac{B\pi}{L}\cos(n\theta)\sum_{s=1}^{\infty} q_s s. \tag{15}$$

The rotation of the plate edge, with a reversed sign, is

$$\left(\frac{\partial w_P}{\partial r}\right)_{r=a} = \cos(n\theta)\sum_{i=0}^{\infty}\tilde{q}_i \frac{\lambda_{ni}}{a}\left[A_{ni}\mathrm{J}_n'(\lambda_{ni}) + C_{ni}\mathrm{I}_n'(\lambda_{ni})\right]. \tag{16}$$

Therefore, by using equations (14)–(16), the maximum potential energy stored in the coupling spring is given by

$$V_{C_{P-S}} = \frac{1}{2}c_1 a\,\psi_n \Bigg\{ B^2 \frac{\pi^2}{L^2}\sum_{s=1}^{\infty}\sum_{j=1}^{\infty} q_s q_j s\, j + \sum_{i=0}^{\infty}\sum_{h=0}^{\infty}\tilde{q}_i\tilde{q}_h \frac{\lambda_{ni}}{a}\frac{\lambda_{nh}}{a}\left[A_{ni}\mathrm{J}_n'(\lambda_{ni}) + C_{ni}\mathrm{I}_n'(\lambda_{ni})\right]$$

$$\times \left[A_{nh}\mathrm{J}_n'(\lambda_{nh}) + C_{nh}\mathrm{I}_n'(\lambda_{nh})\right] - 2B\frac{\pi}{L}\sum_{s=1}^{\infty}\sum_{i=0}^{\infty} q_s\tilde{q}_i\, s\frac{\lambda_{ni}}{a}\left[A_{ni}\mathrm{J}_n'(\lambda_{ni}) + C_{ni}\mathrm{I}_n'(\lambda_{ni})\right]\Bigg\}. \tag{17}$$

The maximum potential energy stored in the distributed translational springs of stiffness k_1 (N/m^2) simulating the junction between the shell and the ring stiffener, located at $x = x^*$, is

$$V_{C_{R-S}} = \frac{1}{2} k_1 \int_0^{2\pi} [(w)_{x=x^*} - w_R]^2 a \, \mathrm{d}\theta$$

$$= \frac{1}{2} k_1 a \psi_n \Bigg[G_n^2 - 2G_n B \sum_{s=1}^{\infty} q_s \sin(s\pi x^*/L)$$

$$+ B^2 \sum_{s=1}^{\infty} \sum_{j=1}^{\infty} q_s q_j \sin(s\pi x^*/L) \sin(j\pi x^*/L) \Bigg]. \tag{18}$$

Obviously, additional stiffeners would be considered in the same way. As a consequence of neglecting the effect of the connection joining the rotation of the shell and the ring in a section through the shell axis, the model is best for rings of small width, where the reciprocal contact area is close to a circle.

The maximum potential energy stored by the Winkler elastic foundation is

$$V_B = \frac{1}{2} k' \int_0^{2\pi} \int_0^a w_P^2 \, r \, \mathrm{d}r \, \mathrm{d}\theta = \frac{1}{2} k' \psi_n a^2 \sum_{i=0}^{\infty} \tilde{q}_i^2, \tag{19}$$

where k' is the stiffness of the foundation (N/m^3).

The effect of a constant in-plane load on the bottom plate can be included in the study without significant complication of the solution. The maximum potential energy associated with flexural vibrations of the bottom plate as a consequence of in-plane load is [51]

$$V_I = \frac{1}{2} N_{ipl} \int_0^{2\pi} \int_0^a \{(\partial w_P/\partial r)^2 + [(1/r)(\partial w_P/\partial \theta)]^2\} r \, \mathrm{d}r \, \mathrm{d}\theta$$

$$= \frac{1}{2} N_{ipl} \psi_n \sum_{i=0}^{\infty} \sum_{h=0}^{\infty} \tilde{q}_i \tilde{q}_h \Bigg[\frac{\lambda_{ni}\lambda_{nh}}{a^2} \int_0^a \Bigg[A_{ni} \mathrm{J}_n'\Big(\lambda_{ni}\frac{r}{a}\Big) + C_{ni} \mathrm{I}_n'\Big(\lambda_{ni}\frac{r}{a}\Big) \Bigg]$$

$$\times \Bigg[A_{nh} \mathrm{J}_n'\Big(\lambda_{nh}\frac{r}{a}\Big) + C_{nh} \mathrm{I}_n'\Big(\lambda_{nh}\frac{r}{a}\Big) \Bigg] r \, \mathrm{d}r + n^2 \int_0^a \Bigg[A_{ni} \mathrm{J}_n\Big(\lambda_{ni}\frac{r}{a}\Big) + C_{ni} \mathrm{I}_n\Big(\lambda_{ni}\frac{r}{a}\Big) \Bigg]$$

$$\times \Bigg[A_{nh} \mathrm{J}_n\Big(\lambda_{nh}\frac{r}{a}\Big) + C_{nh} \mathrm{I}_n\Big(\lambda_{nh}\frac{r}{a}\Big) \Bigg] \frac{\mathrm{d}r}{r} \Bigg\}, \tag{20}$$

where N_{ipl} is the in-plane load for unit length (N/m) ($N_{ipl} > 0$ is traction). The influence of the membrane stress of the shell is not taken into account in this study. This effect was studied, for example, by Chiba [52] and Gonçalves and Ramos [14].

3. DYNAMIC BEHAVIOUR OF THE LIQUID–STRUCTURE INTERACTION

The tank is considered partially filled with an inviscid and incompressible liquid, with a free surface orthogonal to the vertical tank axis; the free surface is at distance H from

the bottom plate (see Figure 1). Surface tension of the liquid and hydrostatic pressure effects are neglected in the present study.

For an incompressible and inviscid liquid the deformation potential satisfies the Laplace equation [22, 43, 53]

$$\nabla^2\phi(r, \theta, x) = 0. \tag{21}$$

The deformation potential ϕ is related to the velocity potential $\tilde{\phi}$ by

$$\tilde{\phi}(r, \theta, x, t) = -\mathrm{i}\omega\phi\ \mathrm{e}^{\mathrm{i}\omega t}, \tag{22}$$

which is assumed to be harmonic; i is the imaginary unit and ω is the natural circular frequency of vibration. The liquid deformation potential, upon using the principle of superposition, can be divided into

$$\phi = \phi^{(1)} + \phi^{(2)} + \phi^{(S)}, \tag{23}$$

where $\phi^{(1)}$ describes the velocity potential of the liquid associated with the flexible shell considering the bottom plate as rigid, $\phi^{(2)}$ describes the velocity potential for the flexible bottom plate considering the shell as rigid, and $\phi^{(S)}$ is due to the sloshing of the liquid in the rigid tank.

The boundary conditions imposed to the liquid for the three complementary boundary value problems are [22, 43, 53]

$$(\partial\phi^{(1)}/\partial x)_{x=0} = 0, \qquad (\partial\phi^{(1)}/\partial r)_{r=a} = w(x, \theta), \qquad (\phi^{(1)})_{x=H} = 0, \tag{24a–c}$$

$$(\partial\phi^{(2)}/\partial x)_{x=0} = -w_P(r, \theta), \qquad (\partial\phi^{(2)}/\partial r)_{r=a} = 0, \qquad (\phi^{(2)})_{x=H} = 0, \tag{25a–c}$$

and

$$(\partial\phi^{(S)}/\partial x)_{x=0} = 0, \qquad (\partial\phi^{(S)}/\partial r)_{r=a} = 0, \qquad g(\partial\phi/\partial x)_{x=H} = \omega^2(\phi)_{x=H}. \tag{26a–c}$$

By using equations (24) and (25), the linearized sloshing condition (26c) can be rewritten as

$$g[\partial(\phi^{(1)} + \phi^{(2)} + \phi^{(S)})/\partial x]_{x=H} = \omega^2(\phi^{(S)})_{x=H}, \tag{27}$$

where g is the gravitational acceleration. It is useful to introduce the Rayleigh quotient [22, 43] in order to determine all the terms that one must compute to obtain the solution of the problem:

$$\omega^2 = \frac{V_S + V_P + V_R + V_{C_{P-S}} + V_{C_{R-S}} + V_I + V_L}{T_S^* + T_P^* + T_R^* + \tilde{T}_L^*}. \tag{28}$$

The only terms that remain to be computed in equation (28) are the reference kinetic energy of the liquid, $\tilde{T}_L^*$, and the maximum potential energy, V_L, of the free surface waves of the liquid itself. Using Green's theorem for harmonic functions [43, 54] gives the reference kinetic energy of the liquid inside the tank as

$$\tilde{T}_L^* = \frac{1}{2}\rho_L \iint_S \phi \frac{\partial\phi}{\partial z}\,\mathrm{d}S = \frac{1}{2}\rho_L \iint_{S_F} \phi \frac{\partial\phi}{\partial z}\,\mathrm{d}S + T_L^*, \tag{29}$$

where ρ_L is the liquid mass density (kg/m^3), z is the direction normal at any point on the boundary surface S of the liquid domain and is pointed outwards, $S = S_1 + S_2 + S_F$, S_1

is the shell lateral surface, S_2 is the plate surface, S_F is the free liquid surface, and the simplified reference kinetic energy T_L^* of the liquid is

$$T_L^* = \frac{1}{2}\rho_L \iint_{S_1+S_2} \phi \frac{\partial \phi}{\partial z}\,\mathrm{d}S = \frac{1}{2}\rho_L \iint_{S_1} \phi \frac{\partial \phi}{\partial r}\,\mathrm{d}S - \frac{1}{2}\rho_L \iint_{S_2} \phi \frac{\partial \phi}{\partial x}\,\mathrm{d}S$$

$$= \frac{1}{2}\rho_L \iint_{S_1} (\phi^{(1)} + \phi^{(2)} + \phi^{(S)}) w\,\mathrm{d}S + \frac{1}{2}\rho_L \iint_{S_2} (\phi^{(1)} + \phi^{(2)} + \phi^{(S)}) w_P\,\mathrm{d}S$$

$$= T_L^{(1)} + T_L^{(1-2)} + T_L^{(1-S)} + T_L^{(2-1)} + T_L^{(2)} + T_L^{(2-S)}. \tag{30}$$

The maximum potential energy V_L of the free surface waves of the liquid is given by [22, 43]

$$V_L = \frac{1}{2}\rho_L g \iint_{S_F} \frac{\partial \phi}{\partial z}\frac{\partial \phi}{\partial z}\,\mathrm{d}S = \frac{1}{2}\rho_L \omega^2 \iint_{S_F} \phi \frac{\partial \phi}{\partial z}\,\mathrm{d}S, \tag{31}$$

where the second equality is obtained by using the sloshing condition, equation (26c). It is interesting to observe that, by using equations (29) and (31), the Rayleigh quotient can be rewritten in the following simplified formulation,

$$\omega^2 = \frac{V_S + V_P + V_R + V_{C_{P-S}} + V_{C_{R-S}} + V_I}{T_S^* + T_F^* + T_R^* + T_L^*}, \tag{32}$$

where the potential energy V_L does not appear; also, it is not necessary to integrate the quantity $\phi(\partial\phi/\partial z)$ over the free surface of the liquid. In conclusion only the additional term T_L^* due to the liquid must still be computed; it is divided into six terms as in equation (30).

3.1. LIQUID–SHELL INTERACTION

In this section, the vibration problem of a simply supported flexible shell of a circular cylindrical tank with a rigid base is considered. A large number of papers on the vibrations of partially fluid-filled shells have been published, e.g., references [8–16, 19–23, 25–28, 32–33].

The liquid deformation potential $\phi^{(1)}$ is assumed to be of the form [33]

$$\phi^{(1)} = \sum_{s=1}^{\infty} q_s \Phi_s^{(1)}. \tag{33}$$

The functions $\Phi_s^{(1)}$ are given by

$$\Phi_s^{(1)}(x, r, \theta) = \sum_{m=1}^{\infty} A_{nsm} \mathrm{I}_n\left(\frac{2m-1}{2}\pi\frac{r}{H}\right)\cos(n\theta)\cos\left(\frac{2m-1}{2}\pi\frac{x}{H}\right), \tag{34}$$

where A_{mns} are coefficients depending on the integers m, n and s. Functions $\Phi_s^{(1)}$ satisfy the Laplace equation and the two boundary conditions given in equations (24b, c); the condition given in equation (24a) is used to compute the coefficients A_{mns}:

$$\sum_{m=1}^{\infty} A_{nsm}\frac{(2m-1)\pi}{2H}\mathrm{I}_n'\left(\frac{2m-1}{2}\pi\frac{a}{H}\right)\cos\left(\frac{2m-1}{2}\pi\frac{x}{H}\right) = B\sin\left(s\pi\frac{x}{L}\right). \tag{35}$$

Equation (35) must be satisfied for all values $0 \leqslant x \leqslant H$. If one multiplies this equation by $\cos(\frac{1}{2}(2j-1)(\pi x/H))$ and then integrates between 0 and H, using the well-known properties of the orthogonal trigonometric functions, one obtains

$$\Phi_s^{(1)} = \sum_{m=1}^{\infty} \frac{4B}{(2m-1)\pi}\,\sigma_{sm}\,\frac{\mathrm{I}_n\left(\dfrac{2m-1}{2}\,\pi\,\dfrac{r}{H}\right)}{\mathrm{I}_n'\left(\dfrac{2m-1}{2}\,\pi\,\dfrac{a}{H}\right)}\cos(n\theta)\cos\left(\frac{2m-1}{2}\,\pi\,\frac{x}{H}\right), \tag{36}$$

where

$$\sigma_{sm} = \frac{\dfrac{s}{L} + (-1)^m\,\dfrac{2m-1}{2H}\sin\left(s\pi\,\dfrac{H}{L}\right)}{\left(\dfrac{s^2}{L^2} - \dfrac{4m^2-4m+1}{4H^2}\right)\pi} \qquad \text{if } s \neq \frac{2m-1}{2}\,\frac{L}{H}, \tag{37a}$$

or

$$\sigma_{sm} = \frac{L}{2s\pi} \qquad \text{if } s = \frac{2m-1}{2}\,\frac{L}{H}. \tag{37b}$$

Therefore, the term $T_L^{(1)}$ of the reference kinetic energy of the liquid is given by

$$T_L^{(1)} = \frac{1}{2}\,\rho_L \int_0^{2\pi}\int_0^{H} (\phi^{(1)})_{r=a}\, wa\,\mathrm{d}\theta\,\mathrm{d}x$$

$$= \frac{1}{2}\,\rho_L B^2 a\,\psi_n \sum_{s=1}^{\infty}\sum_{j=1}^{\infty} q_s q_j \sum_{m=1}^{\infty} \frac{4\sigma_{sm}\sigma_{jm}}{(2m-1)\pi}\,\frac{\mathrm{I}_n\left(\dfrac{2m-1}{2}\,\pi\,\dfrac{a}{H}\right)}{\mathrm{I}_n'\left(\dfrac{2m-1}{2}\,\pi\,\dfrac{a}{H}\right)}. \tag{38}$$

3.2. LIQUID–PLATE INTERACTION

In this section, the vibration problem of the simply supported flexible bottom plate is studied, with the circular cylindrical shell considered to be rigid [1–7].

The liquid deformation potential $\phi^{(2)}$ is assumed to be of the form [7, 33]

$$\phi^{(2)} = \sum_{i=0}^{\infty} \tilde{q}_i \Phi_i^{(2)}. \tag{39}$$

The functions $\Phi_i^{(2)}$, for axisymmetric modes ($n = 0$), are expressed as

$$\Phi_i^{(2)}(r,\theta,x) = K_{0i0}(x-H) + \sum_{k=1}^{\infty} K_{0ik}\mathrm{J}_0(\varepsilon_{0k}r/a)\left[\cosh(\varepsilon_{0k}x/a) - \frac{\sinh(\varepsilon_{0k}x/a)}{\tanh(\varepsilon_{0k}H/a)}\right], \tag{40}$$

and, for asymmetric ($n > 0$) modes, as

$$\Phi_i^{(2)}(x,r,\theta) = \cos(n\theta)\sum_{k=1}^{\infty} K_{nik}\mathrm{J}_n(\varepsilon_{nk}r/a)\left[\cosh(\varepsilon_{nk}x/a) - \frac{\sinh(\varepsilon_{nk}x/a)}{\tanh(\varepsilon_{nk}H/a)}\right], \tag{41}$$

where ε_{nk} are solutions of the equation

$$J'_n(\varepsilon_{nk}) = 0, \qquad k = 1, \ldots \infty, \tag{42}$$

upon rejecting the first solution $\varepsilon = 0$ for $n = 0$. Functions $\Phi_i^{(2)}$ satisfy equations (21) and (25b, c). The constants K_{nik} are calculated in order to satisfy equation (25a). For asymmetric modes,

$$\sum_{k=1}^{\infty} K_{nik} J_n(\varepsilon_{nk} r/a) \frac{\varepsilon_{nk}}{a \tanh(\varepsilon_{nk} H/a)} = [A_{ni} J_n(\lambda_{ni} r/a) + C_{ni} I_n(\lambda_{ni} r/a)]. \tag{43}$$

Equation (43) must be satisfied for all values $0 \leqslant r \leqslant a$. If one multiplies this equation by $(1/a^2)J_n(\varepsilon_{nk} r/a)r$ and integrates between 0 and a, then upon using the orthogonality of the Bessel functions, this results in [7]

$$K_{nik} = \frac{(A_{ni}\beta_{nik} + C_{ni}\gamma_{nik})}{\alpha_{nk}\varepsilon_{nk}} a \tanh\left(\varepsilon_{nk}\frac{H}{a}\right), \tag{44}$$

where, by using equation (42), one has [49]

$$\alpha_{nk} = \frac{1}{a^2}\int_0^a J_n^2\left(\varepsilon_{nk}\frac{r}{a}\right) r \, dr = \frac{1}{2}[1 - (n/\varepsilon_{nk})^2][J_n(\varepsilon_{nk})]^2, \tag{45}$$

$$\beta_{nik} = \frac{1}{a^2}\int_0^a J_n\left(\varepsilon_{nk}\frac{r}{a}\right) J_n\left(\lambda_{ni}\frac{r}{a}\right) r \, dr = \frac{\lambda_{ni}}{\varepsilon_{nk}^2 - \lambda_{ni}^2} J'_n(\lambda_{ni}) J_n(\varepsilon_{nk}), \tag{46}$$

$$\gamma_{nik} = \frac{1}{a^2}\int_0^a J_n\left(\varepsilon_{nk}\frac{r}{a}\right) I_n\left(\lambda_{ni}\frac{r}{a}\right) r \, dr = \frac{\lambda_{ni}}{\varepsilon_{nk}^2 + \lambda_{ni}^2} I'_n(\lambda_{ni}) J_n(\varepsilon_{nk}). \tag{47}$$

Then, the term $T_L^{(2)}$ of the reference kinetic energy of the liquid is given by

$$T_L^{(2)} = \frac{1}{2}\rho_L a^3 \psi_n \sum_{i=0}^{\infty}\sum_{h=0}^{\infty} \tilde{q}_i \tilde{q}_h \sum_{k=1}^{\infty} \frac{(A_{ni}\beta_{nik} + C_{ni}\gamma_{nik})}{\alpha_{nk}\varepsilon_{nk}} (A_{nh}\beta_{nhk} + C_{nh}\gamma_{nhk}) \tanh\left(\varepsilon_{nk}\frac{H}{a}\right). \tag{48}$$

For axisymmetric modes, equation (43) is replaced by

$$-K_{0i0} + \sum_{k=1}^{\infty} K_{0ik} J_0\left(\varepsilon_{0k}\frac{r}{a}\right) \frac{\varepsilon_{0k}}{a \tanh(\varepsilon_{0k} H/a)} = \left[A_{0i} J_0\left(\frac{\lambda_{0i} r}{a}\right) + C_{0i} I_0\left(\frac{\lambda_{0i} r}{a}\right)\right]. \tag{49}$$

The constant K_{0i0} is given by

$$\frac{K_{0i0}}{2} = -\frac{1}{a^2}\int_0^a \left[A_{0i} J_0\left(\lambda_{0i}\frac{r}{a}\right) + C_{0i} I_0\left(\lambda_{0i}\frac{r}{a}\right)\right] r \, dr = -\tau_{0i}, \tag{50}$$

where [49]

$$\tau_{0i} = \left[\frac{A_{0i}}{\lambda_{0i}} J_1(\lambda_{0i}) + \frac{C_{0i}}{\lambda_{0i}} I_1(\lambda_{0i})\right]. \tag{51}$$

The constants K_{0ik}, for $k > 0$, are obtained from equation (44) computed for $n = 0$; therefore, for axisymmetric modes, the term $T_L^{*(2)}$ of the reference kinetic energy of the liquid is given by

$$T_L^{(2)} = \frac{1}{2}\rho_L a^3 \psi_n \sum_{i=0}^{\infty}\sum_{h=0}^{\infty} \tilde{q}_i \tilde{q}_h$$

$$\times \left[2\frac{H}{a}\tau_{0i}\tau_{0h} + \sum_{k=1}^{\infty} \frac{(A_{0i}\beta_{0ik} + C_{0i}\gamma_{0ik})}{\alpha_{0k}\varepsilon_{0k}} (A_{0h}\beta_{0hk} + C_{0h}\gamma_{0hk}) \tanh\left(\varepsilon_{0k}\frac{H}{a}\right)\right]. \tag{52}$$

3.3. SHELL-PLATE INTERACTION VIA THE LIQUID

In equation (30), it was shown that the simplified reference kinetic energy of the liquid T_L^* is not given by the simple sum $T_L^{(1)} + T_L^{(2)} + T_L^{(S-1)} + T_L^{(S-2)}$, but by six terms; this is so because of the coupling effect of the liquid. In fact, even if one eliminated the coupling springs between the plate and the shell, these two elements would remain coupled by the presence of the liquid within the tank. In particular, the quantity $T_L^{(1-2)}$, for asymmetric modes, is given by

$$T_L^{(1-2)} = \frac{1}{2}\rho_L \iint_{S_1} (\phi^{(2)})_{r=a} w \, \mathrm{d}S$$

$$= \frac{1}{2}\rho_L B\, a^2 \psi_n \sum_{s=1}^{\infty}\sum_{i=0}^{\infty} q_s \tilde{q}_i \sum_{k=1}^{\infty} K_{nik} \mathrm{J}_n(\varepsilon_{nk}) \left[\zeta_{nsk}^{(1)} - \frac{\zeta_{nsk}^{(2)}}{\tanh(\varepsilon_{nk}H/a)}\right], \tag{53}$$

where the constants K_{ink} are given by equation (44) and

$$\zeta_{nsk}^{(1)} = \frac{1}{a}\int_0^H \cosh\left(\varepsilon_{nk}\frac{x}{a}\right)\sin\left(\frac{s\pi x}{L}\right)\mathrm{d}x$$

$$= \frac{\dfrac{s\pi a}{L} - \dfrac{s\pi a}{L}\cos\left(\dfrac{s\pi H}{L}\right)\cosh\left(\varepsilon_{nk}\dfrac{H}{a}\right) + \varepsilon_{nk}\sin\left(\dfrac{s\pi H}{L}\right)\sinh\left(\varepsilon_{nk}\dfrac{H}{a}\right)}{\varepsilon_{nk}^2 + \dfrac{s^2\pi^2 a^2}{L^2}}, \tag{54}$$

$$\zeta_{nsk}^{(2)} = \frac{1}{a}\int_0^H \sinh\left(\varepsilon_{nk}\frac{x}{a}\right)\sin\left(\frac{s\pi x}{L}\right)\mathrm{d}x$$

$$= \frac{-\dfrac{s\pi a}{L}\cos\left(\dfrac{s\pi H}{L}\right)\sinh\left(\varepsilon_{nk}\dfrac{H}{a}\right) + \varepsilon_{nk}\sin\left(\dfrac{s\pi H}{L}\right)\cosh\left(\varepsilon_{nk}\dfrac{H}{a}\right)}{\varepsilon_{nk}^2 + \dfrac{s^2\pi^2 a^2}{L^2}}. \tag{55}$$

The quantity $T_L^{(1-2)}$, for asixymmetric modes ($n = 0$), is given by

$$T_L^{(1-2)} = \frac{1}{2}\rho_L B\, a^2 \psi_n \sum_{s=1}^{\infty}\sum_{i=0}^{\infty} q_s \tilde{q}_i \left\{ K_{0i0}\zeta_{0s}^{(0)} + \sum_{k=1}^{\infty} K_{0ik}\mathrm{J}_0(\varepsilon_{0k}) \left[\zeta_{0sk}^{(1)} - \frac{\zeta_{0sk}^{(2)}}{\tanh(\varepsilon_{0k}H/a)}\right]\right\}, \tag{56}$$

where

$$\zeta_{0s}^{(0)} = \frac{1}{a}\int_0^H (x - H)\sin(s\pi x/L)\,\mathrm{d}x = \frac{-(s\pi a/L)H + a\sin(s\pi H/L)}{(s\pi a/L)^2}. \tag{57}$$

The component $T_L^{*(2-1)}$ of the reference kinetic energy of the liquid is given by the following expression for both axisymmetric and asymmetric modes:

$$T_L^{(2-1)} = \frac{1}{2}\rho_L \iint_{S_2} (\phi^{(1)}) w_P \,\mathrm{d}S$$

$$= \frac{1}{2}\rho_L B a^2 \psi_n \sum_{s=1}^{\infty}\sum_{i=0}^{\infty} q_s \tilde{q}_i \sum_{m=1}^{\infty} \frac{4\sigma_{sm}}{(2m-1)\pi \mathrm{I}_n'\left(\dfrac{2m-1}{2}\pi\dfrac{a}{H}\right)} (A_{ni}\xi_{nim}^{(1)} + C_{ni}\xi_{nim}^{(2)}), \tag{58}$$

where the constants σ_{ms} are given by equations (37a, b), and $\xi_{nim}^{(i)}$, for $i = 1, 2$, are [49]:

$$\xi_{nim}^{(1)} = \frac{1}{a^2}\int_0^a \mathrm{I}_n\left(\frac{2m-1}{2}\pi\frac{r}{H}\right)\mathrm{J}_n\left(\lambda_{ni}\frac{r}{a}\right) r\,\mathrm{d}r$$

$$= \frac{\dfrac{2m-1}{2}\pi\dfrac{a}{H}}{\left(\dfrac{2m-1}{2}\pi\dfrac{a}{H}\right)^2 + \lambda_{ni}^2}\,\mathrm{J}_n(\lambda_{ni})\mathrm{I}_n'\left(\frac{2m-1}{2}\pi\frac{a}{H}\right), \tag{59}$$

$$\xi_{nim}^{(2)} = \frac{1}{a^2}\int_0^a \mathrm{I}_n\left(\frac{2m-1}{2}\pi\frac{r}{H}\right)\mathrm{I}_n\left(\lambda_{ni}\frac{r}{a}\right) r\,\mathrm{d}r$$

$$= \frac{\lambda_{ni}\mathrm{I}_n\left(\dfrac{2m-1}{2}\pi\dfrac{a}{H}\right)\mathrm{I}_n'(\lambda_{ni}) - \dfrac{2m-1}{2}\pi\dfrac{a}{H}\,\mathrm{I}_n(\lambda_{ni})\mathrm{I}_n'\left(\dfrac{2m-1}{2}\pi\dfrac{a}{H}\right)}{\lambda_{ni}^2 - \left(\dfrac{2m-1}{2}\pi\dfrac{a}{H}\right)^2}. \tag{60}$$

3.4. SLOSHING OF THE LIQUID AT THE FREE SURFACE

The liquid deformation potential $\phi^{(S)}$ due to the sloshing in a rigid tank for asymmetric modes ($n \geqslant 1$) can be written in the form

$$\phi^{(S)} = \sum_{m=1}^{\infty} F_{nm}\mathrm{J}_n\left(\varepsilon_{nm}\frac{r}{a}\right)\cosh\left(\varepsilon_{nm}\frac{x}{a}\right)\cos(n\theta), \tag{61}$$

where ε_{nm} are solutions of equation (42) and F_{mn} are the parameters of the Ritz expansion of the sloshing modes. The potential $\phi^{(S)}$ satisfies equations (26a, b); then the sloshing

condition, equation (27), must be applied. Using equations (33, 34, 39–41, 61) and eliminating $\cos(n\theta)$, gives

$$\sum_{s=1}^{\infty} q_s \sum_{k=1}^{\infty} Z_{nsk} \mathrm{I}_n\left(\frac{2k-1}{2}\pi\,\frac{r}{H}\right) + \sum_{i=0}^{\infty} \tilde{q}_i \sum_{k=1}^{\infty} W_{nik} \mathrm{J}_n\left(\varepsilon_{nk}\frac{r}{a}\right)$$

$$+ \sum_{m=1}^{\infty} \frac{\varepsilon_{nm}}{a} F_{nm} \mathrm{J}_n\left(\varepsilon_{nm}\frac{r}{a}\right) \sinh\left(\varepsilon_{nm}\frac{H}{a}\right) = \frac{\omega^2}{g} \sum_{m=1}^{\infty} F_{nm} \mathrm{J}_n\left(\varepsilon_{nm}\frac{r}{a}\right) \cosh\left(\varepsilon_{nm}\frac{H}{a}\right), \quad (62)$$

where

$$Z_{nsk} = -\frac{2B}{H}\sigma_{sk} \sin\left(\frac{2k-1}{2}\pi\right) \Big/ \mathrm{I}_n'\left(\frac{2k-1}{2}\pi\,\frac{a}{H}\right), \quad (63)$$

$$W_{nik} = (\varepsilon_{nk}/a) K_{nik} [\sinh(\varepsilon_{nk} H/a) - \cosh(\varepsilon_{nk} H/a)/\tanh(\varepsilon_{nk} H/a)]. \quad (64)$$

Equation (62) must be satisfied for all $0 \leqslant r \leqslant a$. Therefore, by multiplying it by $(1/a^2)\mathrm{J}_n(\varepsilon_{nj} r/a) r$ and integrating between 0 and a, the following sloshing equations are obtained [49],

$$\sum_{s=1}^{\infty} q_s \sum_{k=1}^{\infty} Z_{nsk} \tilde{\xi}_{nmk}^{(1)} + \sum_{i=0}^{\infty} \tilde{q}_i W_{nim} \alpha_{nm} + \frac{\varepsilon_{nm}}{a} F_{nm} \alpha_{nm} \sinh\left(\varepsilon_{nm}\frac{H}{a}\right)$$

$$= \frac{\omega^2}{g} F_{nm} \alpha_{nm} \cosh\left(\varepsilon_{nm}\frac{H}{a}\right), \quad (65)$$

for $m = 1, \ldots, \infty$, where $\tilde{\xi}_{nmk}^{(1)}$ has the same definition as $\xi_{nim}^{(1)}$ in equation (59) but with λ_{ni} replaced by ε_{ni}; α_{nm} is defined in equation (45).

In the case of axisymmetric modes ($n = 0$), $\phi^{(S)}$ can be written in the form

$$\phi^{(S)} = F_{00} + \sum_{m=1}^{\infty} F_{0m} \mathrm{J}_0\left(\varepsilon_{0m}\frac{r}{a}\right) \cosh\left(\varepsilon_{0m}\frac{x}{a}\right), \quad (66)$$

and the equation of sloshing becomes

$$\sum_{s=1}^{\infty} q_s \sum_{k=1}^{\infty} Z_{0sk} \mathrm{I}_0\left(\frac{2k-1}{2}\pi\,\frac{r}{H}\right) + \sum_{i=0}^{\infty} \tilde{q}_i \sum_{k=1}^{\infty} \left[K_{0i0} + W_{0ik} \mathrm{J}_0\left(\varepsilon_{0k}\frac{r}{a}\right)\right]$$

$$+ \sum_{m=1}^{\infty} \frac{\varepsilon_{0m}}{a} F_{0m} \mathrm{J}_0\left(\varepsilon_{0m}\frac{r}{a}\right) \sinh\left(\varepsilon_{0m}\frac{H}{a}\right) = \frac{\omega^2}{g}\left[F_{00} + \sum_{m=1}^{\infty} F_{0m} \mathrm{J}_0\left(\varepsilon_{0m}\frac{r}{a}\right) \cosh\left(\varepsilon_{0m}\frac{H}{a}\right)\right]. \quad (67)$$

Integrating equation (67) with respect to $r\,\mathrm{d}r$ between 0 and a one obtains

$$\sum_{s=1}^{\infty} q_s \sum_{k=1}^{\infty} 2Z_{0sk}\left[\mathrm{I}_1\left(\frac{2k-1}{2}\,\pi\,\frac{a}{H}\right)\Big/\left(\frac{2k-1}{2}\,\pi\,\frac{a}{H}\right)\right] + \sum_{i=0}^{\infty} \tilde{q}_i K_{0i0} = \frac{\omega^2}{g} F_{00}. \tag{68}$$

Then one has the other sloshing equations for $m = 1, \ldots, \infty$, that are obtained by inserting $n = 0$ in equation (65).

3.5. KINETIC ENERGY OF THE LIQUID RELATED TO SLOSHING

The term $T_L^{(1-S)}$ of the kinetic energy of the liquid due to sloshing is

$$T_L^{(1-S)} = \frac{1}{2}\,\rho_L \int_0^{2\pi}\int_0^{H} (\phi^{(S)})_{r=a} w a\,\mathrm{d}x\,\mathrm{d}\theta$$

$$= \frac{1}{2}\,\rho_L a^2 \psi_n B \sum_{s=1}^{\infty}\sum_{m=1}^{\infty} q_s F_{nm} \mathrm{J}_n(\varepsilon_{nm})\zeta_{nsm}^{(1)} \qquad \text{for } n \geqslant 1 \tag{69a}$$

$$= \frac{1}{2}\,\rho_L a^2 \psi_0 B \sum_{s=1}^{\infty} q_s \left\{F_{00}\,\frac{L[1-\cos(s\pi H/L)]}{s\pi a} + \sum_{m=1}^{\infty} F_{0m}\mathrm{J}_0(\varepsilon_{0m})\zeta_{0sm}^{(1)}\right\}$$

$$\text{for } n = 0. \tag{69b}$$

The term $T_L^{(2-S)}$ of the kinetic energy of the liquid due to sloshing is

$$T_L^{(2-S)} = \frac{1}{2}\,\rho_L \int_0^{2\pi}\int_0^{a} (\phi^{(S)})_{x=0}\, w_P r\,\mathrm{d}r\,\mathrm{d}\theta$$

$$= \frac{1}{2}\,\rho_L a^2 \psi_n \sum_{i=0}^{\infty}\sum_{m=1}^{\infty} \tilde{q}_i F_{nm}(A_{ni}\beta_{nim} + C_{ni}\gamma_{nim}) \qquad \text{for } n \geqslant 1 \tag{70a}$$

$$= \frac{1}{2}\,\rho_L a^2 \psi_0 \sum_{i=0}^{\infty} \tilde{q}_i \left[F_{00}\tau_{0i} + \sum_{m=1}^{\infty} F_{0m}(A_{0i}\beta_{0im} + C_{0i}\gamma_{0im})\right] \quad \text{for} \quad n = 0. \tag{70b}$$

4. THE EIGENVALUE PROBLEM INCLUDING THE SLOSHING CONDITION

For the numerical calculation of the natural frequencies and the parameters of the Ritz expansion of modes, only N terms in the expansion of w, equation (1), $\tilde{N} + 1$ terms in the expansion of w_P, equation (4), and $\tilde{\tilde{N}}$ in the expansion of $\phi^{(S)}(\tilde{\tilde{N}} + 1$ in the case of axisymmetric modes), equation (61), are considered, where N, $\tilde{N}$ and $\tilde{\tilde{N}}$ are chosen large enough to give the required accuracy to the solution. So, all the energies are given by finite summations. It is convenient to introduce a vectorial notaion. The vector $\mathbf{q}$ of the parameters of the Ritz expansions is defined by

$$\mathbf{q} = \begin{Bmatrix} G_n \\ \{q\} \\ \{\tilde{q}\} \\ \{F\} \end{Bmatrix}, \tag{71}$$

where the coefficient G_n is defined in equation (9) and

$$\{q\} = \begin{Bmatrix} q_1 \\ \vdots \\ q_N \end{Bmatrix}, \qquad \{\tilde{q}\} = \begin{Bmatrix} \tilde{q}_0 \\ \vdots \\ \tilde{q}_{\tilde{N}} \end{Bmatrix} \quad \text{and} \quad \{F\} = \begin{Bmatrix} F_{n1} \\ \vdots \\ F_{n\tilde{N}} \end{Bmatrix}. \tag{72}$$

For axisymmetric ($n = 0$) modes, the coefficient F_{00} must also be included in the vector $\{F\}$.

The maximum potential energy of the shell, equation (11), becomes

$$V_S = \tfrac{1}{2}\psi_n \mathbf{q}^T \mathbf{K}_S \mathbf{q}. \tag{73}$$

The partitioned matrix $\mathbf{K}_S$ is

$$\mathbf{K}_S = \begin{bmatrix} 0 & \{\mathbf{0}\}^T & \{\mathbf{0}\}^T & \{\mathbf{0}\}^T \\ \{\mathbf{0}\} & [\mathbf{E}_S] & [\mathbf{0}] & [\mathbf{0}] \\ \{\mathbf{0}\} & [\mathbf{0}] & [\mathbf{0}] & [\mathbf{0}] \\ \{\mathbf{0}\} & [\mathbf{0}] & [\mathbf{0}] & [\mathbf{0}] \end{bmatrix}, \tag{74}$$

where the elements of the diagonal submatrix $[\mathbf{E}_S]$ are given by

$$[\mathbf{E}_S]_{sj} = \delta_{sj}\rho_s h_S a(L/2)B^2\omega_s^2, \qquad s, j = 1, \ldots, N, \tag{75}$$

and δ_{sj} is the Kronecker delta.

The maximum potential energy of the bottom plate, equation (12), can be written as

$$V_P = \tfrac{1}{2}\psi_n \mathbf{q}^T \mathbf{K}_P \mathbf{q}. \tag{76}$$

The matrix $\mathbf{K}_P$ is

$$\mathbf{K}_P = \begin{bmatrix} 0 & \{\mathbf{0}\}^T & \{\mathbf{0}\}^T & \{\mathbf{0}\}^T \\ \{\mathbf{0}\} & [\mathbf{0}] & [\mathbf{0}] & [\mathbf{0}] \\ \{\mathbf{0}\} & [\mathbf{0}] & [\mathbf{E}_P] & [\mathbf{0}] \\ \{\mathbf{0}\} & [\mathbf{0}] & [\mathbf{0}] & [\mathbf{0}] \end{bmatrix}, \tag{77}$$

where the elements of the diagonal submatrix $[\mathbf{E}_P]$ are given by

$$[\mathbf{E}_P]_{ih} = \delta_{ih}(D/a^2)\lambda_{ni}^4, \qquad i, h = 0, \ldots, \tilde{N}. \tag{78}$$

The maximum potential energy of the ring-stiffener, equation (13), may be written as

$$V_R = \tfrac{1}{2}\psi_n \mathbf{q}^T \mathbf{K}_R \mathbf{q}. \tag{79}$$

The matrix $\mathbf{K}_R$ is

$$\mathbf{K}_R = \begin{bmatrix} e_n & \{\mathbf{0}\}^T & \{\mathbf{0}\}^T & \{\mathbf{0}\}^T \\ \{\mathbf{0}\} & [\mathbf{0}] & [\mathbf{0}] & [\mathbf{0}] \\ \{\mathbf{0}\} & [\mathbf{0}] & [\mathbf{0}] & [\mathbf{0}] \\ \{\mathbf{0}\} & [\mathbf{0}] & [\mathbf{0}] & [\mathbf{0}] \end{bmatrix}, \tag{80}$$

where $e_n = \rho_R h_R L_R a\, \omega_{R_n}^2 (1 + K_x n^2/a^2)$.

The maximum potential energy stored by the rotational coupling spring that joins the plate to the shell, equation (17), can be written as

$$V_{C_{P-S}} = \tfrac{1}{2}\psi_n \mathbf{q}^T \mathbf{K}_{P-S} \mathbf{q}. \tag{81}$$

The matrix $\mathbf{K}_{P-S}$ is

$$\mathbf{K}_{P-S} = \begin{bmatrix} 0 & \{\mathbf{0}\}^T & \{\mathbf{0}\}^T & \{\mathbf{0}\}^T \\ \{\mathbf{0}\} & [\mathbf{K}_1] & [\mathbf{K}_2] & [\mathbf{0}] \\ \{\mathbf{0}\} & [\mathbf{K}_2]^T & [\mathbf{K}_3] & [\mathbf{0}] \\ \{\mathbf{0}\} & [\mathbf{0}] & [\mathbf{0}] & [\mathbf{0}] \end{bmatrix}, \tag{82}$$

where the elements of the submatrices $[\mathbf{K}_i]$ are given in Appendix A.

The maximum potential energy stored by the translational coupling spring that joints the ring-stiffener to the shell, equation (18), can be written as

$$V_{C_{R-S}} = \tfrac{1}{2}\psi_n \mathbf{q}^T \mathbf{K}_{R-S} \mathbf{q}. \tag{83}$$

The matrix $\mathbf{K}_{R-S}$ is

$$\mathbf{K}_{R-S} = \begin{bmatrix} k_1 a & \{\tilde{\mathbf{K}}_1\}^T & \{\mathbf{0}\}^T & \{\mathbf{0}\}^T \\ \{\tilde{\mathbf{K}}_1\} & [\tilde{\mathbf{K}}_2] & [\mathbf{0}] & [\mathbf{0}] \\ \{\mathbf{0}\} & [\mathbf{0}] & [\mathbf{0}] & [\mathbf{0}] \\ \{\mathbf{0}\} & [\mathbf{0}] & [\mathbf{0}] & [\mathbf{0}] \end{bmatrix}, \tag{84}$$

where the elements of the vector $\{\tilde{\mathbf{K}}_1\}$ and of the matrix $[\tilde{\mathbf{K}}_2]$ are given in Appendix A.

The maximum potential energy stored by the Winkler elastic foundation, equation (19), may be written as

$$V_B = \tfrac{1}{2}\psi_n \mathbf{q}^T \mathbf{K}_B \mathbf{q}, \tag{85}$$

where

$$\mathbf{K}_B = \begin{bmatrix} 0 & \{\mathbf{0}\}^T & \{\mathbf{0}\}^T & \{\mathbf{0}\}^T \\ \{\mathbf{0}\} & [\mathbf{0}] & [\mathbf{0}] & [\mathbf{0}] \\ \{\mathbf{0}\} & [\mathbf{0}] & [\mathbf{E}_B] & [\mathbf{0}] \\ \{\mathbf{0}\} & [\mathbf{0}] & [\mathbf{0}] & [\mathbf{0}] \end{bmatrix}, \tag{86}$$

in which $[\mathbf{E}_B] = k'a[\mathbf{I}]$, and $[\mathbf{I}]$ is the identity $(\tilde{N}+1) \times (\tilde{N}+1)$ submatrix.

The maximum potential energy stored by the bottom plate as a consequence of the in-plane load, equation (20), is

$$V_I = \tfrac{1}{2}\psi_n \mathbf{q}^T \mathbf{K}_I \mathbf{q}, \tag{87}$$

where

$$\mathbf{K}_I = \begin{bmatrix} 0 & \{\mathbf{0}\}^T & \{\mathbf{0}\}^T & \{\mathbf{0}\}^T \\ \{\mathbf{0}\} & [\mathbf{0}] & [\mathbf{0}] & [\mathbf{0}] \\ \{\mathbf{0}\} & [\mathbf{0}] & [\mathbf{E}_L] & [\mathbf{0}] \\ \{\mathbf{0}\} & [\mathbf{0}] & [\mathbf{0}] & [\mathbf{0}] \end{bmatrix}, \tag{88}$$

and, for $i, j = 0, \ldots, \tilde{N}$

$$[\mathbf{E}_L]_{ih} = N_{ipl}\frac{\lambda_{ni}\lambda_{nh}}{a^2}\int_0^a \left[A_{ni}\mathrm{J}'_n\left(\lambda_{ni}\frac{r}{a}\right) + C_{ni}\mathrm{I}'_n\left(\lambda_{ni}\frac{r}{a}\right)\right]\left[A_{nh}\mathrm{J}'_n\left(\lambda_{nh}\frac{r}{a}\right) + C_{nh}\mathrm{I}'_n\left(\lambda_{nh}\frac{r}{a}\right)\right] r\,\mathrm{d}r$$

$$+ n^2\int_0^a \left[A_{ni}\mathrm{J}_n\left(\lambda_{ni}\frac{r}{a}\right) + C_{ni}\mathrm{I}_n\left(\lambda_{ni}\frac{r}{a}\right)\right]\left[A_{nh}\mathrm{J}_n\left(\lambda_{nh}\frac{r}{a}\right) + C_{nh}\mathrm{I}_n\left(\lambda_{nh}\frac{r}{a}\right)\right]\frac{\mathrm{d}r}{r}. \qquad (89)$$

The reference kinetic energy of the shell, equation (7), and of the plate, equation (8), may be written as

$$T_S^* = \tfrac{1}{2}\psi_n \mathbf{q}^T\mathbf{M}_S\mathbf{q}, \qquad T_P^* = \tfrac{1}{2}\psi_n \mathbf{q}^T\mathbf{M}_P\mathbf{q}, \qquad (90, 91)$$

respectively, where

$$\mathbf{M}_S = \begin{bmatrix} 0 & \{\mathbf{0}\}^T & \{\mathbf{0}\}^T & \{\mathbf{0}\}^T \\ \{\mathbf{0}\} & [\mathbf{H}_S] & [\mathbf{0}] & [\mathbf{0}] \\ \{\mathbf{0}\} & [\mathbf{0}] & [\mathbf{0}] & [\mathbf{0}] \\ \{\mathbf{0}\} & [\mathbf{0}] & [\mathbf{0}] & [\mathbf{0}] \end{bmatrix}, \qquad \mathbf{M}_P = \begin{bmatrix} 0 & \{\mathbf{0}\}^T & \{\mathbf{0}\}^T & \{\mathbf{0}\}^T \\ \{\mathbf{0}\} & [\mathbf{0}] & [\mathbf{0}] & [\mathbf{0}] \\ \{\mathbf{0}\} & [\mathbf{0}] & [\mathbf{H}_P] & [\mathbf{0}] \\ \{\mathbf{0}\} & [\mathbf{0}] & [\mathbf{0}] & [\mathbf{0}] \end{bmatrix}, \qquad (92, 93)$$

where $[\mathbf{H}_S] = \rho_S h_S a(L/2)B^2[\mathbf{I}]$, $[\mathbf{H}_P] = \rho_P h_P a^2[\mathbf{I}]$, and $[\mathbf{I}]$ is the $N \times N$ identity submatrix in $\mathbf{M}_S$ and $[\mathbf{I}]$ is the $(\tilde{N}+1)\times(\tilde{N}+1)$ identity submatrix in $\mathbf{M}_P$.

The reference kinetic energy of the ring-stiffener, equation (10) can be written as

$$T_R^* = \tfrac{1}{2}\psi_n \mathbf{q}^T\mathbf{M}_R\mathbf{q}, \qquad (94)$$

The matrix $\mathbf{M}_R$ is

$$\mathbf{M}_B = \begin{bmatrix} h_{ring} & \{\mathbf{0}\}^T & \{\mathbf{0}\}^T & \{\mathbf{0}\}^T \\ \{\mathbf{0}\} & [\mathbf{0}] & [\mathbf{0}] & [\mathbf{0}] \\ \{\mathbf{0}\} & [\mathbf{0}] & [\mathbf{0}] & [\mathbf{0}] \\ \{\mathbf{0}\} & [\mathbf{0}] & [\mathbf{0}] & [\mathbf{0}] \end{bmatrix}, \qquad (95)$$

where $h_{ring} = \rho_R h_R L_R a(1 + K_x n^2/a^2)$.

The simplified reference kinetic energy of the liquid, that was previously divided into six different contributions in equation (30), can be written as

$$T_L^* = \tfrac{1}{2}\psi_n \mathbf{q}^T\mathbf{M}_L\mathbf{q}, \qquad (96)$$

where $\mathbf{M}_L$ is a symmetric partitioned matrix of dimension $(1 + N + (\tilde{N} + 1) + \tilde{\tilde{N}}) \times (1 + N + (\tilde{N} + 1) + \tilde{\tilde{N}})$:

$$\mathbf{M}_L = \begin{bmatrix} 0 & \{\mathbf{0}\}^T & \{\mathbf{0}\}^T & \{\mathbf{0}\}^T \\ \{\mathbf{0}\} & [\mathbf{M}_1] & [\mathbf{M}_2] & [\mathbf{M}_{S1}] \\ \{\mathbf{0}\} & [\mathbf{M}_2]^T & [\mathbf{M}_3] & [\mathbf{M}_{S2}] \\ \{\mathbf{0}\} & [\mathbf{0}] & [\mathbf{0}] & [\mathbf{0}] \end{bmatrix}, \tag{97}$$

in which the elements of the submatrices $[\mathbf{M}_i]$ and $[\mathbf{M}_{Si}]$ are given in Appendix B.

The sloshing condition, equation (65), is given by

$$[[\mathbf{E}_1], [\mathbf{E}_2], [\mathbf{E}_3]] \begin{Bmatrix} \{q\} \\ \{\tilde{q}\} \\ \{F\} \end{Bmatrix} = \omega^2 \quad [[\mathbf{0}], [\mathbf{0}], [\mathbf{H}_1]] \begin{Bmatrix} \{q\} \\ \{\tilde{q}\} \\ \{F\} \end{Bmatrix}, \tag{98}$$

where $[\mathbf{E}_1]$ has dimension $\tilde{\tilde{N}} \times N$, $[\mathbf{E}_2]$ has dimension $\tilde{\tilde{N}} \times (\tilde{N} + 1)$ and $[\mathbf{E}_3]$ and $[\mathbf{H}_1]$ have dimension $\tilde{\tilde{N}} \times \tilde{\tilde{N}}$; these matrices are given by

$$[\mathbf{E}_1]_{ij} = g \sum_{k=1}^{\infty} Z_{njk} \tilde{\xi}^{(1)}_{nik}, \qquad i = 1, \ldots, \tilde{\tilde{N}} \qquad \text{and} \qquad j = 1, \ldots, N, \tag{99a}$$

$$[\mathbf{E}_2]_{ij} = g W_{nji} \alpha_{ni}, \qquad i = 1, \ldots, \tilde{\tilde{N}} \qquad \text{and} \qquad j = 1, \ldots, \tilde{N} + 1, \tag{99b}$$

$$[\mathbf{E}_3]_{ij} = g \delta_{ij} \alpha_{ni} (\varepsilon_{ni}/a) \sinh (\varepsilon_{ni} H/a), \quad [\mathbf{H}_1]_{ij} = \delta_{ij} \alpha_{ni} \cosh (\varepsilon_{ni} H/a),$$

$$i, j = 1, \ldots, \tilde{\tilde{N}}. \tag{99c, d}$$

For axisymmetric modes, the dimension $\tilde{\tilde{N}}$ of all the matrices must be changed into $\tilde{\tilde{N}} + 1$. The additional row of the four non-zero matrices involved in the sloshing condition for $n = 0$ is (see equation (68))

$$[\mathbf{E}_1]_{0j} = 2g \sum_{k=1}^{\infty} Z_{0jk} \mathrm{I}_1\left(\frac{2k-1}{2} \pi \frac{a}{H}\right) \Big/ \left(\frac{2k-1}{2} \pi \frac{a}{H}\right), \qquad j = 1, \ldots, N + 1, \tag{100a}$$

$$[\mathbf{E}_2]_{0j} = -2g\tau_{0j}, \qquad j = 1, \ldots, \tilde{N} + 1, \tag{100b}$$

$$[\mathbf{E}_3]_{0j} = 0, \qquad [\mathbf{H}_1]_{0j} = \delta_{0j}, \qquad j = 1, \ldots, \tilde{\tilde{N}} + 1. \tag{100c, d}$$

The values of the vector $\mathbf{q}$ of the parameters of the Ritz expansion are determined in order to render the Rayleigh quotient of equation (32) stationary [23, 43], by inserting in

the eigenvalue problem also the sloshing condition that determines the value of the coefficients F_{nm} [14, 43]; then the following Galerkin equation is obtained:

$$\begin{bmatrix} e_n + k_1 a & \{\tilde{\mathbf{K}}_1\}^T & \{\mathbf{0}\}^T & \{\mathbf{0}\}^T \\ \{\tilde{\mathbf{K}}_1\} & [\mathbf{E}_S] + [\mathbf{K}_1] + [\tilde{\mathbf{K}}_2] & [\mathbf{K}_2] & [\mathbf{0}] \\ \{\mathbf{0}\} & [\mathbf{K}_2]^T & [\mathbf{E}_P] + [\mathbf{K}_3] + [\mathbf{E}_B] + [\mathbf{E}_L] & [\mathbf{0}] \\ \{\mathbf{0}\} & [\mathbf{E}_1] & [\mathbf{E}_2] & [\mathbf{E}_3] \end{bmatrix} \mathbf{q}$$

$$- \Lambda^2 \begin{bmatrix} h_{ring} & \{\mathbf{0}\}^T & \{\mathbf{0}\}^T & \{\mathbf{0}\}^T \\ \{\mathbf{0}\} & [\mathbf{H}_S] + [\mathbf{M}_1] & [\mathbf{M}_2] & [\mathbf{M}_{S1}] \\ \{\mathbf{0}\} & [\mathbf{M}_2]^T & [\mathbf{H}_P] + [\mathbf{M}_3] & [\mathbf{M}_{S2}] \\ \{\mathbf{0}\} & [\mathbf{0}] & [\mathbf{0}] & [\mathbf{H}_1] \end{bmatrix} \mathbf{q} = 0. \tag{101}$$

Here Λ is the circular frequency of the tank partially filled with liquid. Equation (101) gives a linear eigenvalue problem for a real, non-symmetric matrix.

5. PRESSURE DISTRIBUTION AND WAVE HEIGHT

The pressure exerted by the liquid at a point of the tank wall can be computed by using the linearized Bernoulli equation:

$$(p)_{point} = -\rho_L (\partial \tilde{\phi}/\partial t)_{point} = \rho_L \omega^2 (\phi)_{point}\, \mathrm{e}^{\mathrm{i}\omega t}. \tag{102}$$

This relation allows one to compute the pressure load on the tank wall as a consequence of the sloshing of the liquid inside due to an excitation (e.g., an earthquake or acceleration of a rocket) or due to vibrations. It is also of interest to compute the height of the free surface waves of both sloshing and bulging modes and to compare them to the wall displacements. When the eigenvalue problem is solved and the wall relative displacements are obtained, it is only necessary to compute the function [1]

$$\eta(t) = -(1/g)(\partial \tilde{\phi}/\partial t)_{x=H} = (\omega^2/g)(\phi^{(S)})_{x=H}\, \mathrm{e}^{\mathrm{i}\omega t} = [(\partial \phi)/(\partial x)]_{x=H}\, \mathrm{e}^{\mathrm{i}\omega t} \tag{103}$$

to obtain the relative displacement η of the free surface. As a consequence of the linearized free surface boundary condition (26c) used, only small amplitude waves can correctly be studied.

6. NUMERICAL RESULTS AND DISCUSSION

Numerical results are carried out by solving numerically the eigenvalue problem and using the computer software *Mathematica* [55]. The results obtained are compared to the sloshing circular frequencies in the rigid tank computed by using the formula [1]

$$\omega^2 = g(\varepsilon_{nm}/a) \tanh(\varepsilon_{nm} H/a), \tag{104}$$

and to the bulging frequencies computed when neglecting free surface waves and imposing $\phi = 0$ at the free surface, obtained by Amabili [7, 33]. Equation (104) can easily be obtained by substituting equation (61) into the sloshing condition, equation (26c).

6.1. FLEXIBLE SHELL WITH RIGID BOTTOM

The first case studied is that of a simply supported circular cylindrical shell closed by a rigid bottom and partially filled with water having a mass density $\rho_L = 1000\ \mathrm{kg/m^3}$. It

TABLE 1

Circular frequencies (rad/s) *of sloshing modes of the shell with rigid bottom, filled with water to* $H = 21{\cdot}6$ m; *axisymmetric modes* ($n = 0$)

Mode	Present study Flexible shell	Present study Rigid tank	Kondo [8]	Gupta and Hutchinson [10]
1	1·2244	1·2246	1·2238	1·2244
2	1·6591	1·6592	1·6582	1·6591
3	1·9980	1·9980	1·9969	1·9979
4	2·2865	2·2865	2·2853	2·2864
5	2·5422	2·5423	2·5409	2·5422

TABLE 2

Circular frequencies (rad/s) *of bulging modes of the shell with rigid bottom, filled with water to* $H = 21{\cdot}6$ m; *axisymmetric modes* ($n = 0$)

Mode	Present study Flexible shell	Kondo [8]	Neglecting free surface waves [33]	Gupta and Hutchinson [10]
1	22·244	22·096	22·228	22·349
2	44·010	43·762	44·004	44·170
3	57·191	56·829	57·187	58·244
4	67·291	66·888	67·288	69·513
5	75·850	75·347	75·847	79·189

TABLE 3

Circular frequencies (rad/s) *of sloshing and bulging modes of the shell with rigid bottom, filled with water to* $H = 21{\cdot}6$ m; *modes with four nodal diameters* ($n = 4$)

	Sloshing modes		Bulging modes	
Mode	Present study Flexible shell	Present study Rigid tank	Present study Flexible shell	Neglecting free surface waves [33]
1	1·4425	1·4444	13·658	13·640
2	1·9081	1·9085	34·441	34·434
3	2·2305	2·2308	49·692	49·688
4	2·5027	2·5029	61·877	61·874
5	2·7444	2·7445	71·804	71·802

is clear that to simulate a simple support at the shell-plate joint, it is necessary to use a stiffness $c_1 = 0$ of the rotational coupling spring. Solutions for this particular case are obtained from the global eigenvalue problem while using a very high stiffness of the bottom plate; no shell stiffeners are considered in this case. In order to also have a comparison with results published by others, the following dimensions and material properties of the shell are taken: radius $a = 25$ m, shell height $L = 30$ m, water depth $H = 21{\cdot}6$ m, shell thickness $h_S = 0{\cdot}03$ m; the shell considered is made of a steel with: Young's modulus $E = 206$ GPa, mass density $\rho_S = 7850$ kg/m^3 and Poisson's ratio $\nu = 0{\cdot}3$. The Flügge shell theory is applied to find the natural frequencies of the empty shell.

In Table 1 the sloshing (where the displacement is mainly that of the free surface) frequencies of axisymmetric modes ($n = 0$) are given and compared to those obtained by Kondo [8] and Gupta and Hutchinson [10] for the same shell, and to the results obtained when assuming the shell to be rigid and using equation (104). In Table 2 the bulging (where the shell wall moves the liquid) frequencies of axisymmetric modes ($n = 0$) are given and compared to the results obtained by Kondo [8] and Gupta and Hutchinson [10] for the same shell, as well as to the results obtained by Amabili [30] when neglecting the influence

TABLE 4

Natural frequencies (Hz) *of bulging modes of the cylinder of Gonçalves and Ramos* [14] *empty and completely filled with water*; *only the first mode for each number n of nodal diameters is reported*

	Empty			Water-filled		
n	Present study (Flügge)	Reference [14] (Sanders)	Experiment reference [14]	Present study (Flügge)	Theory reference [14] (Sanders)	Experiment reference [14]
8	278·8	281·4	278	117·2	119	120
9	286·1	288·3	290	125·9	128	124
10	315·5	317·5	334	144·6	146	146
11	360·3	362·2	362	171·2	173	182

TABLE 5

Natural circular frequencies (rad/s) *of sloshing and bulging axisymmetric modes* ($n = 0$) *of the clamped bottom plate with* $h_P = 6{\cdot}604$ mm, $D = 1810{\cdot}75$ N m *in a rigid cylinder water-filled to* $H = 0{\cdot}0635$ m

	Sloshing modes			Bulging modes	
Mode	Present study Flexible plate	Bhuta and Koval [1]	Present study Rigid tank	Present study Flexible plate	Neglecting free surface waves [7, 33]
1	2·300	2·299	2·367	31·03	29·19
2	4·263	4·262	4·274	115·0	114·5
3	6·067	6·066	6·070	260·2	260·0
4	7·741	7·739	7·742	469·6	469·5
5	9·280	9·278	9·281	748·3	748·2

TABLE 6

Natural circular frequencies (rad/s) *of sloshing and bulging axisymmetric modes* ($n = 0$) *of the clamped bottom plate with* $h_P = 6{\cdot}604$ mm, $D = 5432{\cdot}44$ N m *in a rigid cylinder water-filled at* $H = 0{\cdot}0635$ m

	Sloshing modes			Bulging modes	
Mode	Present study Flexible plate	Bhuta and Koval [1]	Present study Rigid tank	Present study Flexible plate	Neglecting free surface waves [7, 33]
1	2·342	2·342	2·367	49·02	47·87
2	4·270	4·269	4·274	188·6	188·3
3	6·069	6·068	6·070	428·2	428·1
4	7·742	7·740	7·742	774·2	774·1
5	9·280	9·278	9·281	1235	1235

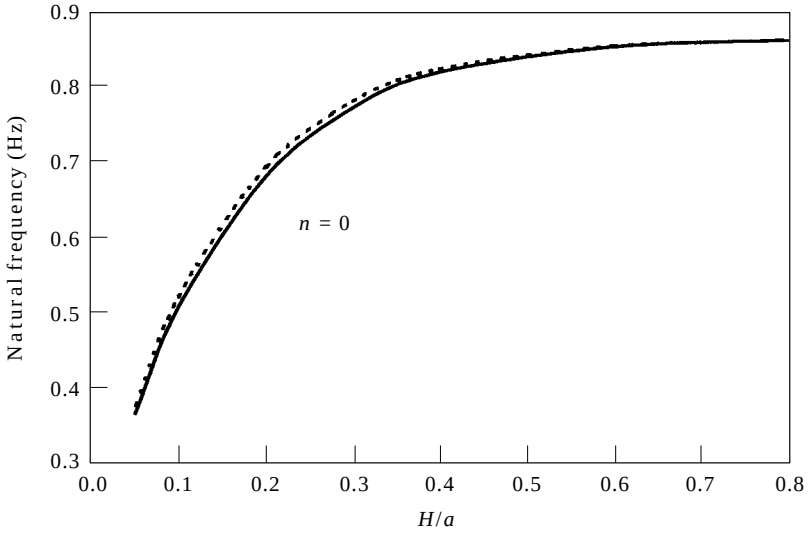

Figure 2. Natural frequency of the first axisymmetric ($n = 0$) sloshing mode of the plate with $D = 1810{\cdot}75$ N m versus the filling ratio H/a. ——, Flexible bottom; - - - , rigid tank.

of the free surface waves: that is, assuming $\phi = 0$ at the free water surface. It is interesting to note that the present results are very close to those obtained by Kondo [8] who has included the free surface waves effect in his theory (it is also observed that not all the signficant figures reported by Kondo could be truly significant, as verified by comparing the present results to those reported in reference [8] for the simple case of sloshing in a rigid tank; moreover Kondo used the Goldenveizer theory of shells). However, the present results are also very close to those obtained by using equation (104) for sloshing modes or neglecting the free surface waves, as reported by Amabili [33]. Moreover, the agreement with the results obtained by Gupta and Hutchinson [10] by using approximate formulae based on variational principles is remarkable.

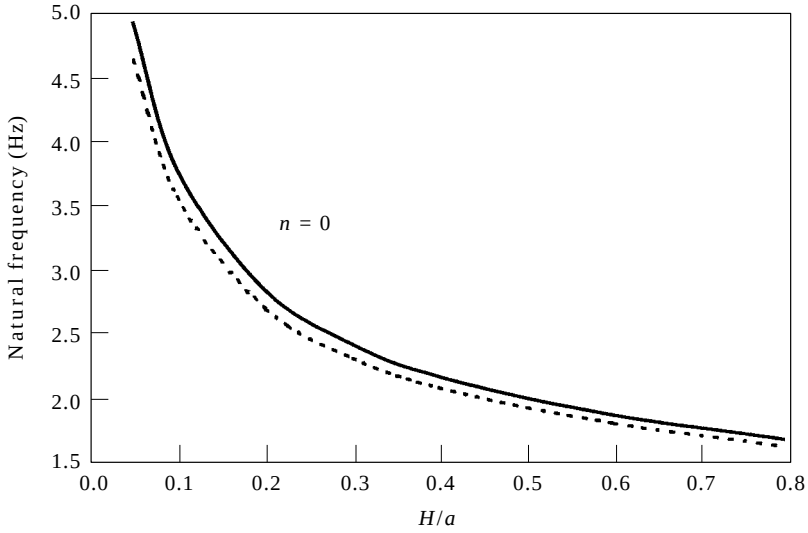

Figure 3. Natural frequency of the first axisymmetric ($n = 0$) bulging mode of the plate with $D = 1810{\cdot}75$ N m versus the filling ratio H/a. ——, Present theory; - - - - , neglecting free surface waves.

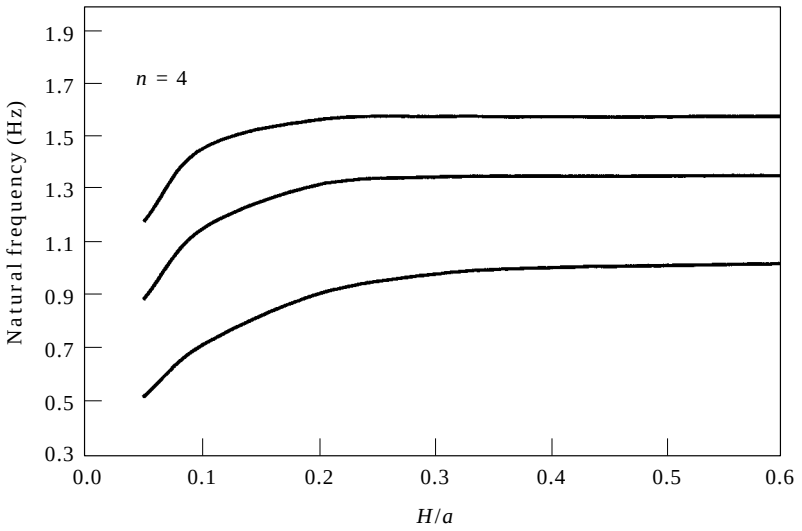

Figure 4. Natural frequency of the first three sloshing modes with four nodal diameters ($n = 4$) of the plate with $D = 1810{\cdot}75$ N m versus the filling ratio H/a.

In Table 3 the sloshing and bulging modes for $n = 4$ of the same shell are reported and compared to the results of equation (104) and to the results obtained when neglecting free surface waves, respectively. In this case differences still remain very small, but they are more significant than for axisymmetric modes ($n = 0$). It was found that for a very low filling ratio (e.g., $H = 1$ m) these differences become negligible. However, what is observed in many cases is that the natural frequencies of the sloshing modes in a rigid shell are higher than those in a flexible shell. The natural frequencies of bulging modes when neglecting the free surface waves ($\phi = 0$) are lower than those when this effect is included; in fact, when one assumes $\phi = 0$ at the free surface, a stronger constraint is imposed on liquid

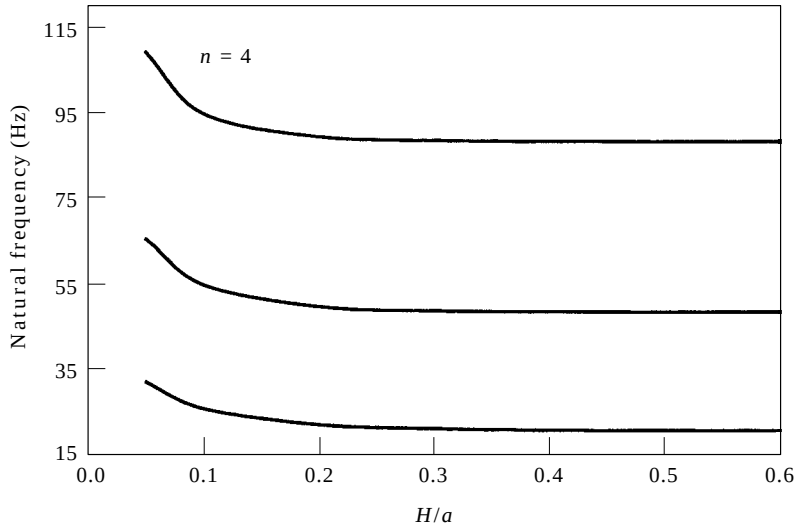

Figure 5. Natural frequency of the first three bulging modes with four nodal diameters ($n = 4$) of the plate with $D = 1810{\cdot}75$ N m versus the filling ratio H/a.

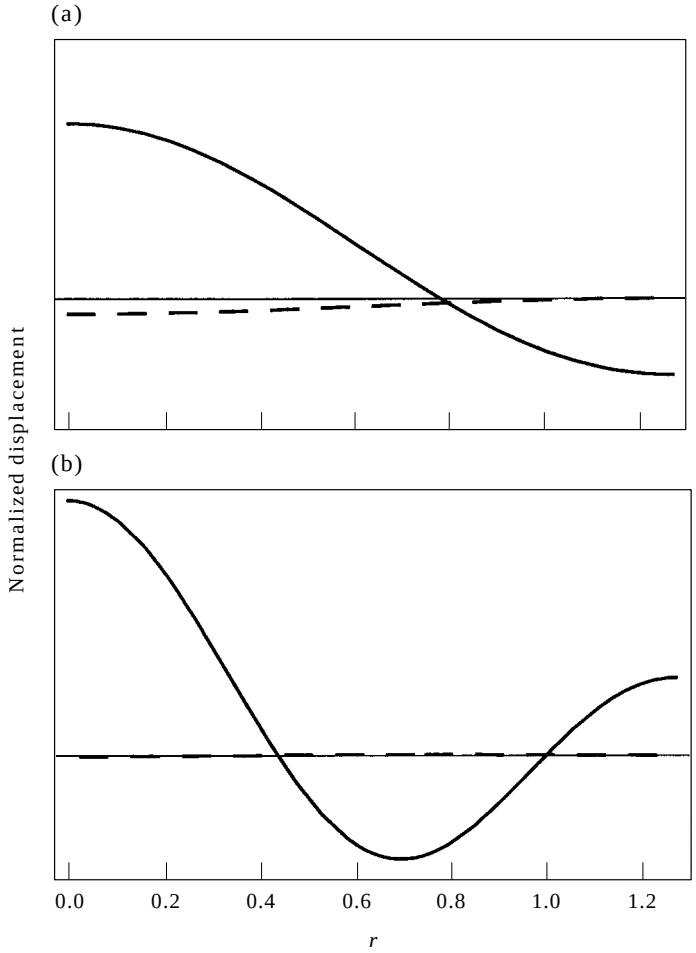

Figure 6. Axisymmetric sloshing modes ($n = 0$) of the free surface (——) and bottom plate (- - -), for $D = 1810{\cdot}75$ N m and $H = 0{\cdot}0635$ m. Both the displacements are measured with respect to the horizontal line. (a) First mode, natural frequency 0·366 Hz; (b) second mode, natural frequency 0·679 Hz.

movement with respect to the sloshing condition, so that the added mass of the liquid when neglecting the free surface effect is larger. Moreover, it was observed that differences between sloshing and bulging modes computed by using simplified theories (e.g., equation (104) or neglecting the free surface waves) and by using the present theory decrease with the number of axial half-waves for each value of n.

Numerical results were also obtained for the simply supported cylinder with a rigid bottom, partially filled with water, studied by Gonçalves and Ramos [14]; they used the Sanders theory of shells instead of the Flügge theory, taking free surface waves into account; experimental results are also available. The following dimensions and material properties of the shell are taken: $a = 0{\cdot}3015$ m, $L = H = 0{\cdot}41$ m, $h_S = 0{\cdot}001$ m, $E = 210$ GPa, $\rho_S = 7850$ kg/m^3 and $\nu = 0{\cdot}3$. The comparison of the bulging frequencies obtained by the present study with experimental and numerical results reported in reference [14] is made in Table 4. Agreement in this case is also quite good.

6.2. FLEXIBLE BOTTOM PLATE AND RIGID CYLINDER

The second special case that can be studied by using the present theory is that of a vertical tank comprising a rigid cylinder and a flexible, circular bottom plate; neither in-plane loading nor an elastic foundation are considered in this section. The following dimensions and material properties of the plate are assumed: $a = 1{\cdot}27$ m, $h_P = 6{\cdot}604$ mm, $H = 0{\cdot}0635$ m, $\rho_P = 3656$ kg/m^3. The liquid inside the tank is water ($\rho_L = 1000$ kg m^{-3}). These parameters correspond to the case studied by Bhuta and Koval [1]. The results for the axisymmetric modes ($n = 0$) of the clamped plate in Tables 5 and 6 compare favourably with the data obtained by Bhuta and Koval [1]; comparison with circular frequencies of sloshing in a rigid tank is also given. In Table 5 the plate considered has a flexural stiffness $D = 1810{\cdot}75$ N m, while in Table 6 the flexural stiffness is increased about three times to $D = 5432{\cdot}44$ N m. Bulging modes obtained when taking into account or neglecting the free surface waves are also given for the two cases. In Table 5 both the first sloshing and the first bulging modes show a significant change in natural frequency with respect to the results of approximate methods. This difference decreases in Table 6, as a consequence of the bottom plate having a larger flexural rigidity. However, differences between the first bulging mode computed when neglecting or accounting for the effect of the free surface waves are still quite significant in Table 6, despite the flexural rigidity of the plate having been increased.

In Figures 2 and 3 the effect of the filling ratio H/a on the natural frequencies of the first axisymmetric ($n = 0$) sloshing and bulging mode, respectively, is investigated for the plate with $D = 1810{\cdot}75$ N m. The results obtained for the first sloshing mode in a tank with

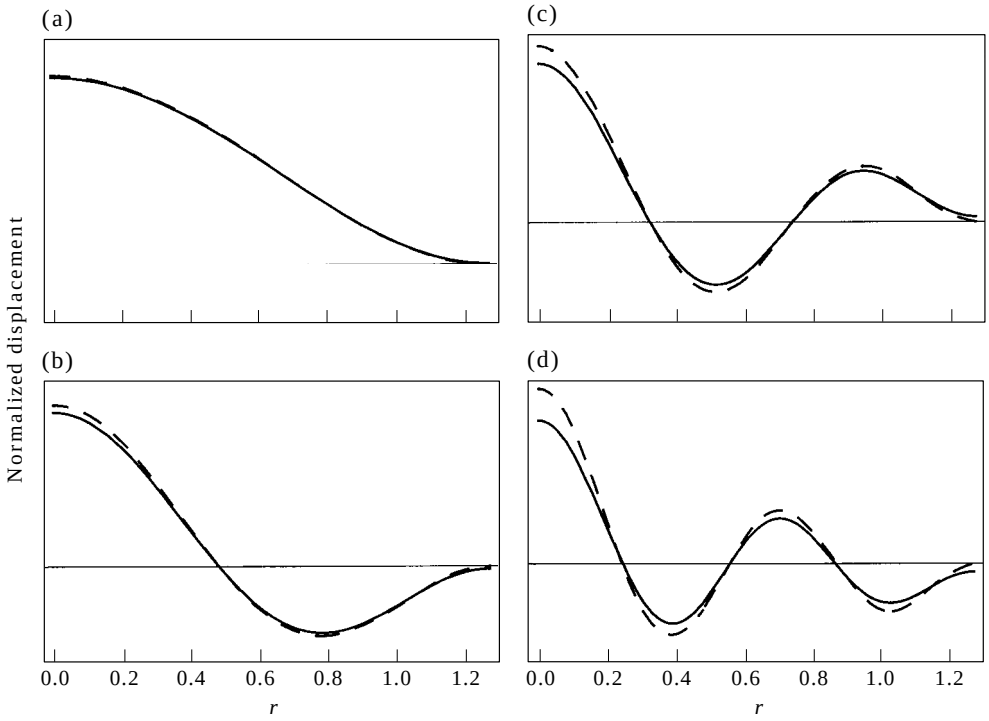

Figure 7. Axisymmetric bulging modes ($n = 0$) of the free surface (——) and bottom plate (- - -), for $D = 1810{\cdot}75$ N m and $H = 0{\cdot}0635$ m. (a) First mode, natural frequency 4·94 Hz; (b) second mode, natural frequency 18·3 Hz; (c) third mode, natural frequency 41·4 Hz; (d) fourth mode, natural frequency 74·7 Hz.

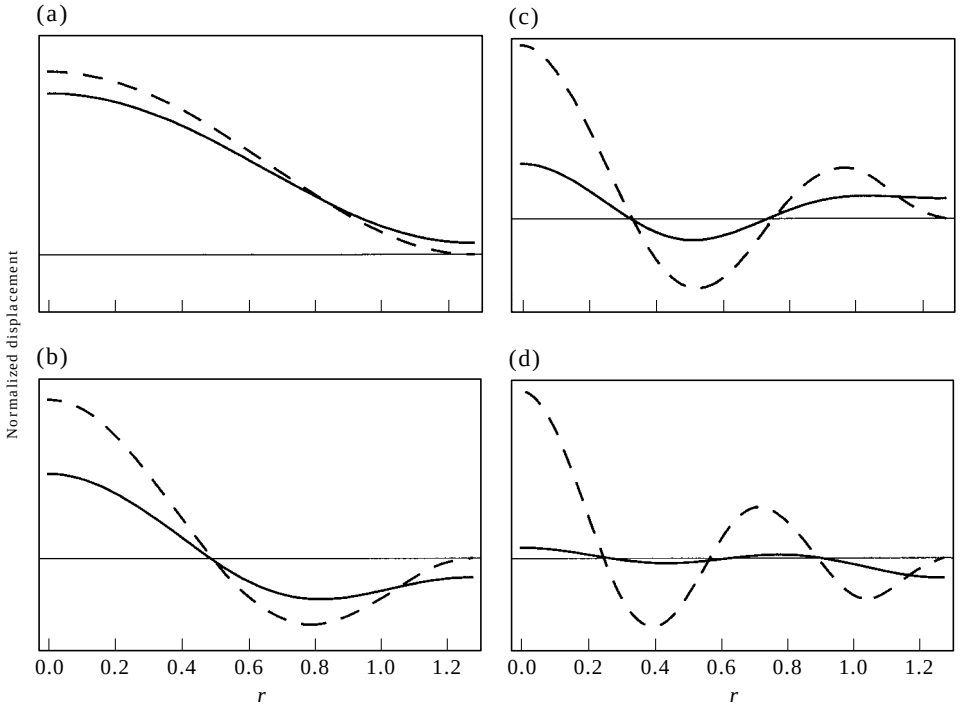

Figure 8. Axisymmetric bulging modes ($n = 0$) of the free surface (——) and bottom plate (- - -), for $D = 1810{\cdot}75$ N m and $H = 0{\cdot}253$ m. (a) First mode, natural frequency 2·84 Hz; (b) second mode, natural frequency 11·7 Hz; (c) third mode, natural frequency 29·2 Hz; (d) fourth mode, natural frequency 57·6 Hz.

a flexible bottom are shown in Figure 2, and they are compared to those of a tank with a rigid bottom; similarly the results for the first bulging mode are compared in Figure 3 to those obtained when neglecting the free surface waves. It is shown that in both cases, the approximate results are not too far from those of the more refined theory. It is interesting to see that the differences between the approximate and exact results decrease as the filling ratio increases.

Similar results are shown in Figures 4 and 5 for modes having four nodal diameters ($n = 4$). In this case the first three sloshing and bulging modes are considered and the comparison with approximate results is not reported because the differences are then very small. Numerical results for asymmetric modes seem not to be available in the literature, so that these results may be considered quite interesting.

In Figures 6–8, the axisymmetric ($n = 0$) mode shapes of both the bottom plate and the free surface are plotted along a radius, so that the relative amplitudes can be compared for each mode. Such data also is not available in the literature. In particular, in Figures 6 and 7 the sloshing and bulging modes, respectively, of the plate with flexural stiffness $D = 1810{\cdot}75$ N m are shown for a filling height $H = 0{\cdot}0635$ m. The first sloshing mode shows that a significant displacement of the bottom plate is associated with the movement of the free surface; but already the second mode shows a negligible displacement. On the contrary, a movement of the free surface comparable to that of the plate is observed for bulging modes; however, the possibility of the free surface following the bottom displacement decreases with mode number and with filling ratio. This last fact is made clear by Figure 8, which shows bulging modes of the same plate for an increased water height of $H = 0{\cdot}253$ m.

TABLE 7

Natural frequencies (Hz) *of bulging axisymmetric modes* ($n = 0$) *of the clamped bottom plate with* $h_P = 2$ mm *in a partially water-filled rigid cylinder*

	$H/a = 0{\cdot}5$		$H/a = 1$	
Mode	Present study	Chiba [5]	Present study	Chiba [5]
1	118	114	95	91
2	568	538	540	513
3	1466	1424	1441	1402

A comparison is then given with respect to the theoretical results of Chiba [5] for bulging modes of a circular bottom plate clamped to a rigid circular cylindrical shell. Chiba's results were obtained by considering the static deflection as well as in-plane forces in the bottom plate due to the liquid weight; in the present results these effects are neglected. However, constant in-plane forces can easily be considered in the present analysis by using equations (87) and (88). The plate dimensions are: $a = 0{\cdot}144$ m, $h_P = 2$ mm and the plate material is a steel, with $E = 206$ GPa, $\rho_P = 7850$ kg/m^3 and $v = 0{\cdot}25$ [5]. The natural frequencies of axisymmetric bulging modes ($n = 0$) are compared in Table 7 and good agreement is obtained. It must be noted that for this case the effect of the in-plane forces and static deflection is not very signficant; however, for other cases studied by Chiba [5], where plates are very thin, these effects are important.

A further satisfactory comparison is given in Figure 9 with the experimental bulging modes obtained by Amabili and Dalpiaz [56] for a simply supported steel plate having the following characteristics: $h_p = 3$ mm, $a = 0{\cdot}1$ m, $E = 206$ GPa, $\rho_P = 7800$ kg/m^3 and $v = 0{\cdot}3$. The modes having no nodal diameter ($n = 0$) and zero (excluding the edge) inner

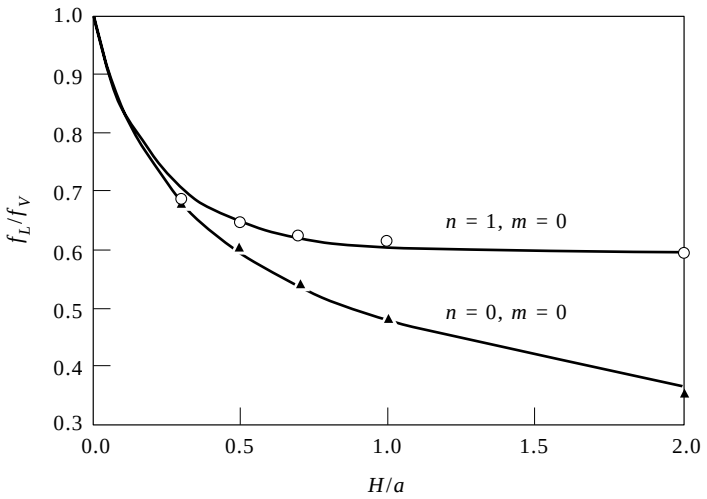

Figure 9. Ratio between the natural frequency of the bottom plate in a partially water-filled tank with rigid shell, f_L, and the frequency of the same plate in vacuum, f_V, versus the filling ratio H/a. Comparison of the present theoretical results (——) with the experiments (○, ▲) of Amabili and Dalpiaz [56] for a simply supported circular plate.

TABLE 8

Natural frequencies (Hz) *of the first three sloshing and bulging modes having* $n = 4$ *nodal diameters of the flexible tank studied in section* 7.3 *for* $H = 0{\cdot}5$ m *and* $n = 4$; *they are obtained by using a different number of terms* $N = \tilde{N} + 1 = \tilde{\tilde{N}}$ *in the expansions of* w, w_P *and* $\phi^{(S)}$

Number of terms	Sloshing			Bulging		
	1st mode	2nd mode	3rd mode	1st mode	2nd mode	3rd mode
2	1·004	1·347	—	25·83	77·24	244
4	1·004	1·347	1·575	22·46	52·98	83·08
6	1·004	1·347	1·575	20·89	48·94	83·02
8	1·004	1·347	1·575	19·86	46·72	82·94
10	1·004	1·347	1·575	19·19	45·45	82·92

circles ($m = 0$) and one nodal diameter and zero nodal inner circle ($n = 1$ and $m = 0$) are considered for different levels of water inside the tank. In Figure 9 the quantity f_L is the natural frequency with liquid inside, whereas f_V is the natural frequency *in vacuo*.

It is of interest to observe that the conditions of a rigid shell can be obtained by the present theory by giving a very high value to the Young's modulus of the shell ($E \to \infty$).

6.3. FLEXIBLE BOTTOM PLATE AND SHELL

In this section, the tank considered is made up of a flexible shell with a flexible bottom; i.e., both components are flexible. No ring stiffeners are considered here. The following dimensions and material properties are taken: $a = 1{\cdot}27$ m, $L = 1$ m, $h_P = 6{\cdot}604$ mm, $h_S = 3$ mm, $\rho_P = \rho_S = 3656$ kg/m^3, $E = 68{\cdot}65$ GPa and $v = 0{\cdot}3$ The same material (aluminium) is assumed for the shell and the bottom plate. The dimensions and material of the bottom plate correspond to the case studied by Bhuta and Koval [1], and also studied in section 6.2, for $D = 1810{\cdot}75$ N m, but now with the shell also flexible. No other

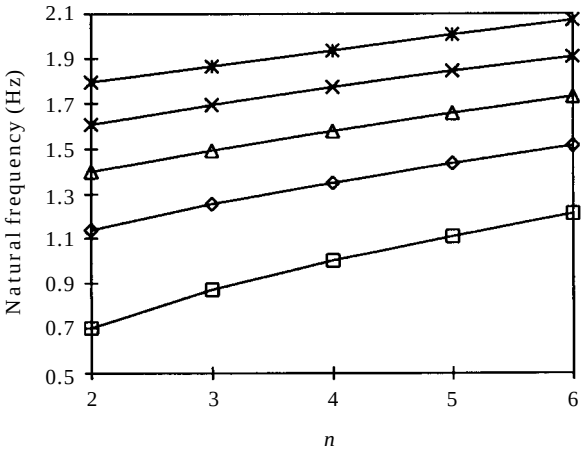

Figure 10. Natural frequencies of sloshing modes of the flexible tank studied in section 6.3 for $H = 0{\cdot}5$ m as a function of the number of nodal diameters n. –□–, First mode; –◇–, second mode; –△–, third mode; – × –, fourth mode; –∗–, fifth mode.

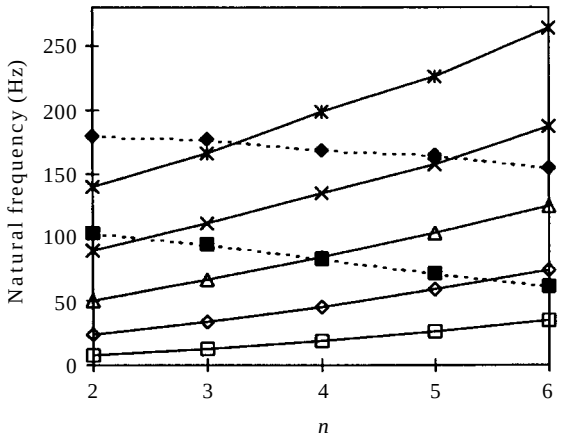

Figure 11. Natural frequencies of bulging modes of the flexible tank studied in section 6.3 for $H = 0{\cdot}5$ m as a function of the number of nodal diameters n. P = plate-dominant modes; S = shell-dominant modes. –□–, First P mode; –◇–, second P mode; –△–, third P mode; – × –, fourth P mode; –∗–, fifth P mode; - -■- -, first S mode; - -◆- -, second S mode.

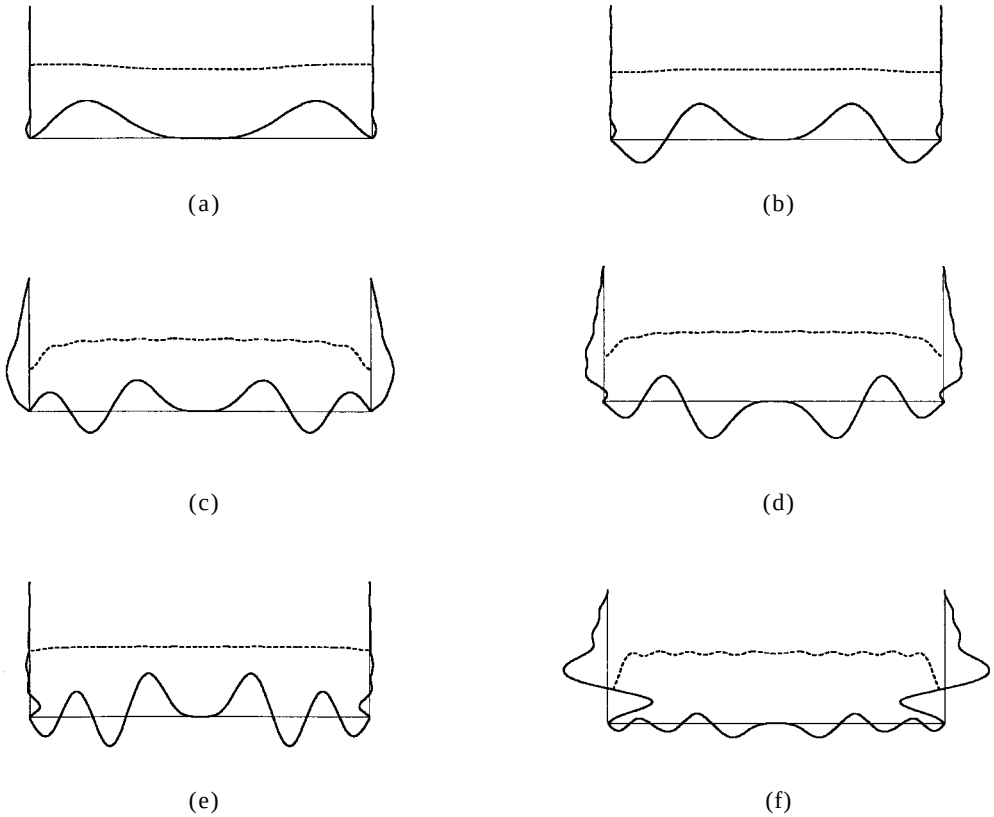

Figure 12. Mode shapes of the first six bulging modes of the flexible tank studied in section 6.3 for $H = 0{\cdot}5$ m and $n = 4$: - - -, moving free surface. (a) First P mode, frequency 19·2 Hz; (b) second P mode, frequency 45·5 Hz; (c) first S mode, frequency 82·9 Hz; (d) third P mode, frequency 84·1 Hz; (e) fourth P mode, frequency 134 Hz; (f) second S mode, frequency 167·8 Hz.

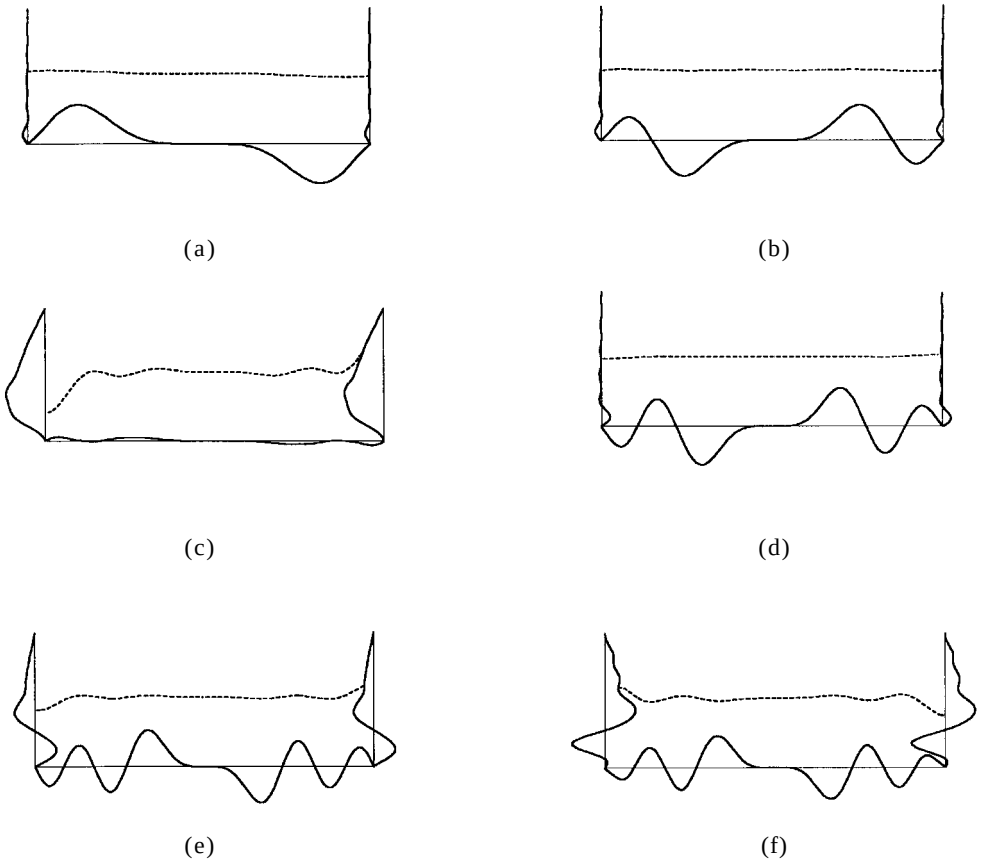

Figure 13. Mode shapes of the first six bulging modes of the flexible tank studied in section 6.3 for $H = 0{\cdot}5$ m and $n = 5$: - - -, moving free surface. (a) First P mode, frequency 26·8 Hz; (b) second P mode, frequency 58·7 Hz; (c) first S mode, frequency 71·9 Hz; (d) third P mode, frequency 102·9 Hz; (e) fourth P mode, frequency 156·6 Hz; (f) second S mode, frequency 164·7 Hz.

theoretical results are available for this kind of tank, excluding those obtained by Amabili [33, 43], but only for bulging modes and with the effect of free surface waves neglected.

Initially a water height $H = 0{\cdot}5$ m is considered. Table 8 shows the convergence of the method as the number of terms in the series expansions is increased; it is seen that ten terms give sufficient accuracy for this application. It was also observed that more terms are necessary to describe accurately the plate dynamics with respect to the terms necessary for the shell. However, for low liquid levels and in case of some shell stiffeners, more terms could be necessary to describe the shell dynamics. In Figures 10 and 11 the natural frequencies of sloshing and bulging modes, respectively, are plotted versus the number of nodal diameters n. It is interesting that, even though we are studying a completely flexible structure, it is still possible to recognize modes dominated by the plate displacement (P) or by the shell displacement (S). This is well illustrated in Figure 12 where the shapes of bulging modes with four nodal diameters ($n = 4$) are represented in a cross-section. In Figure 12(a, b, e) are shown plate-dominant modes, while in Figure 12(f) is plotted a shell-dominant mode. In Figure 12(c, d) are seen modes where the vibration amplitude of the shell has nearly the same magnitude as that of the plate. However, one can say that in Figure 12(c) one has a mode that is "derived from" a mode of the shell, while in

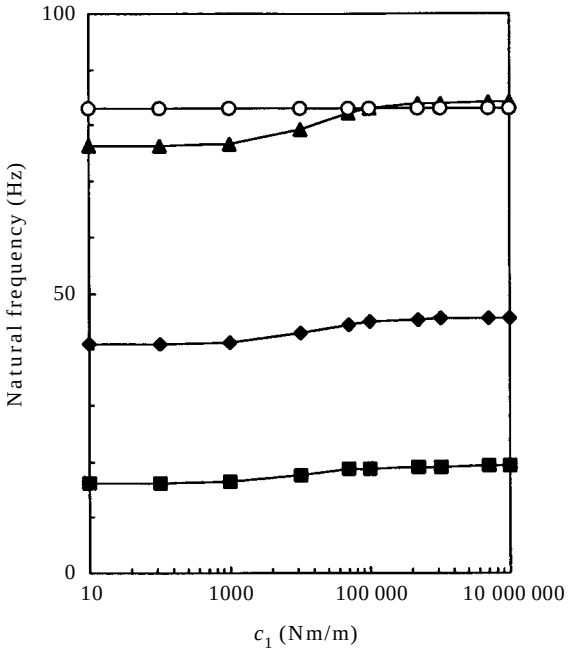

Figure 14. Effect of the coupling spring stiffness c_1 on the natural frequencies of bulging modes of the flexible tank studied in section 6.3 for $H = 0{\cdot}5$ m and $n = 4$. –■–, First P mode; –◆–, second P mode; –▲–, third P mode; –○– first S mode.

Figure 12(d) the mode is derived from the plate. In Figure 12 the displacement of the free surface is given in the same scale as that of the wall displacement.

Figure 13 gives the shapes of bulging modes with five nodal diameters ($n = 5$). In this case one has antisymmetric shapes in a cross-section as a consequence of n being odd, while for n even one has symmetric shapes, as in Figure 12.

The effect of the stiffness of the rotational spring c_1, used to model the joint between the plate and the shell, on the natural frequencies of bulging modes for $H = 0{\cdot}5$ m and $n = 4$ is illustrated in Figure 14. It is interesting to see that a stiffness $c_1 = 10^6$–10^7 well simulates zero relative rotation between the plate and the shell (in the previous numerical computations $c_1 = 5 \times 10^6$ had been assumed). The minimum value of c_1 that assures a rigid connection between plate and shell depends on the rigidity of plate and shell, so that it is different for any given application. In Figure 15 the natural frequencies of bulging modes for $H = 0{\cdot}5$ m and $n = 4$ are plotted versus the stiffness k' of the elastic foundation. Figure 15 shows that plate-dominant modes are more sensitive to k', as expected. Sloshing modes are not very sensitive to changes in c_1 and k' in this case.

The numerical relevance of the coupling between the plate and the shell via the water is illustrated in Table 9, showing differences of a few percent for some modes. However, for bulging modes, the coupling effect via the liquid seems to be more significant than the effect of free surface waves, for a sufficient liquid level. Results in Table 9, obtained when neglecting the coupling via the liquid medium, have been computed by imposing $[\mathbf{M}_2] = [\mathbf{M}_2]^T = \mathbf{0}$ in equations (97, 101).

In Table 10 a comparison of results (bulging modes) of the present study is made with those obtained when (i) neglecting the effect of the free surface waves, (ii) considering the bottom plate rigid and the shell flexible, and (iii) considering the bottom plate flexible and

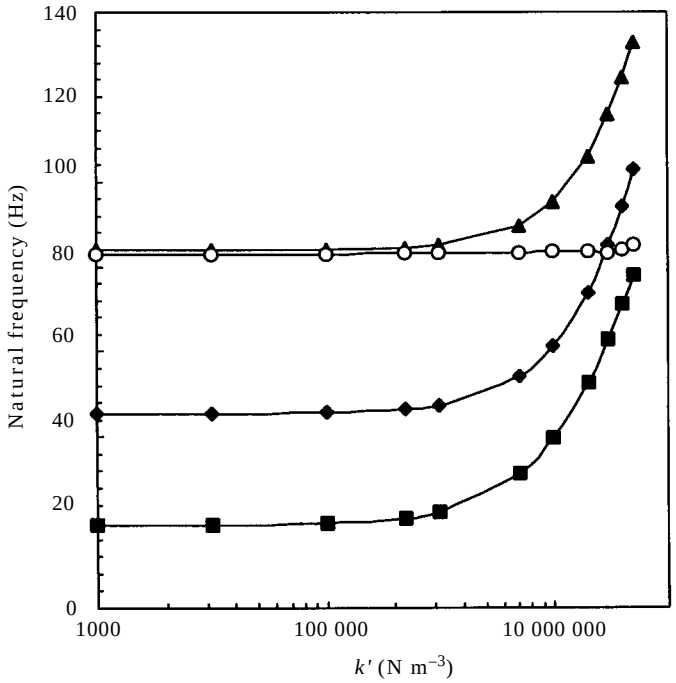

Figure 15. Effect of the foundation stiffness k' on the natural frequencies of bulging modes of the flexible tank studied in section 6.3 for $H = 0{\cdot}5$ m and $n = 4$. –■–, First P mode; –◆–, second P mode; –▲–, third P mode; –○– first S mode.

the shell rigid; in cases (ii) and (iii) the effect of free surface waves was retained. It is evident that, for the tank studied, good accuracy is obtained only by considering both components (base plate and shell) flexible. The approximation of rigid base plate commonly used in practice is accurate only for a very rigid base plate or a base plate on rigid foundation. In the case of a rigid bottom plate, the effect of the spring stiffness c_1 is very important; in fact it changes the boundary condition of the shell at the base from simply supported ($c_1 = 0$) to clamped ($c_1 \to \infty$). For all the data presented in Table 10, $c_1 = 5 \times 10^6$ was taken.

TABLE 9

Natural frequencies (Hz) *of bulging modes of the flexible tank studied in section* 6.3 *for* $H = 0{\cdot}5$ m *and* $n = 4$; *comparison of results of the present study with those obtained neglecting the coupling between the plate and the shell via the water*

Mode	Present study	Neglecting coupling via water
1	19·19	19·07
2	45·45	44·86
3	82·92	78·93
4	84·07	86·28
5	134·00	131·40
6	167·80	166·80

TABLE 10

Natural frequencies (Hz) *of bulging modes of the flexible tank studied in section* 6.3 *for* $H = 0{\cdot}5$ m *and* $n = 4$; *comparison of results of the present study with those obtained when* (*i*) *neglecting the effect of the free surface waves*, (*ii*) *considering the bottom plate rigid and the shell flexible*, (*iii*) *considering the bottom plate flexible and the shell rigid*

Mode	Present study	Neglecting free surface waves	Rigid bottom	Rigid shell
1	19·19	19·19	—	21·69
2	45·45	45·45	—	50·99
3	82·92	82·92	83·74	—
4	84·07	84·07	—	93·36
5	134·00	134·00	—	149·85
6	167·80	167·80	169·90	—

In this case, the frequencies of sloshing modes are not significantly affected by tank flexibility and hence data are not reported here.

A water height $H = 0{\cdot}15$ m is considered next. The natural frequencies computed by using the present theory are compared to those obtained for sloshing in a rigid tank or neglecting the effect of free surface waves in Table 11. It is interesting to see that for this configuration no significant differences are found. The shapes of bulging modes with four nodal diameters ($n = 4$) are drawn in Figure 16 for this water height and can be compared to those shown in Figure 12. As a consequence of the decreased water level, the shell displacement is small for the lowest modes.

6.4. FLEXIBLE TANK WITH RING STIFFENER

For the sake of simplicity, in this section numerical results are given only for tanks with one stiffener. The same tank as studied in section 6.3 is considered. The ring stiffener has the same radius as the tank, a thickness of 0·05 m, a width of 0·03 m and is made of steel having the following characteristics: $E_R = 206$ GPa, $\rho_R = 7850$ kg/m^3 and $\nu_R = 0{\cdot}3$. The first six mode shapes are shown in Figure 17 for $H = 0{\cdot}5$ m, $x^* = 0{\cdot}5$ m and $n = 4$; they can be compared to those in Figure 12 for the same tank and water level, but without the stiffener. It is interesting to note that shell-dominant modes experience significant

TABLE 11

Natural frequencies (Hz) *of sloshing and bulging modes of the flexible tank studied in section* 6.3 *for* $H = 0{\cdot}15$ m *and* $n = 4$; *comparison of results of the present study with those obtained for sloshing in a rigid tank or neglecting the effect of free surface waves*

	Sloshing modes		Bulging modes	
Mode	Present study	Rigid tank	Present study	Neglecting free surface waves
1	0·7605	0·7611	22·94	22·92
2	1·204	1·205	49·72	49·71
3	1·498	1·498	87·52	87·52

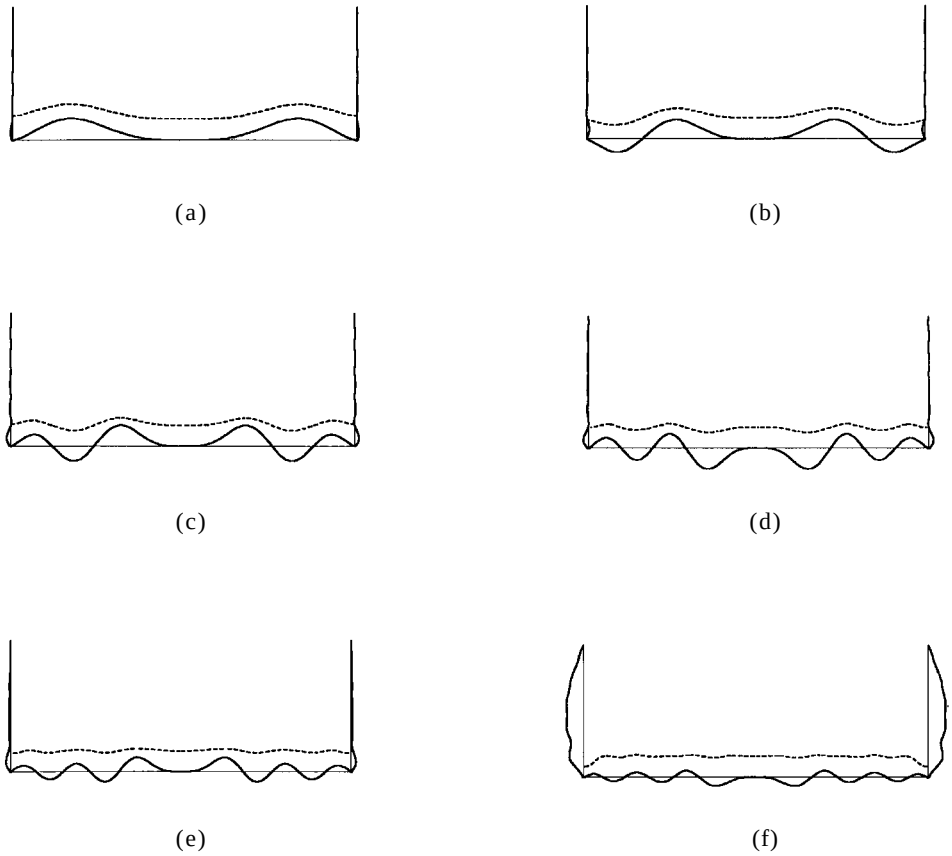

Figure 16. Mode shapes of the first six bulging modes of the flexible tank studied in section 6.3 for $H = 0{\cdot}15$ m and $n = 4$: - - -, moving free surface. (a) First P mode, frequency 22·94 Hz; (b) second P mode, frequency 49·72 Hz; (c) third P mode, frequency 87·52 Hz; (d) fourth P mode, frequency 137·3 Hz; (e) fifth P mode, frequency 198·8 Hz; (f) first S mode, frequency 254·8 Hz.

modifications in shape and minor changes in frequency, while plate-dominant modes are very little affected by the presence of the stiffener.

The percentage change of natural frequencies as a result of the introduction of the ring stiffener is shown in Figure 18 plotted versus the ring position x^*. The first shell-dominant mode is greatly affected by the introduction of one stiffener, and its natural frequency can be significantly increased. Plate-dominant modes are mainly affected by a stiffener located very close to the base. Similar graphs are very useful for the design of tanks and for choosing the best position of the stiffener(s) from a dynamic point of view.

7. CONCLUSIONS

A new and versatile theory has been presented for the dynamics of cylindrical shell-tanks with a flexible bottom and ring stiffeners. Unlike in other extant theories, neither the bottom plate nor the tank itself are considered to be rigid, and free surface waves are taken into account, so that both bulging and sloshing modes of the system may be calculated. The first set of calculations conducted was for the purpose of validation of the theory,

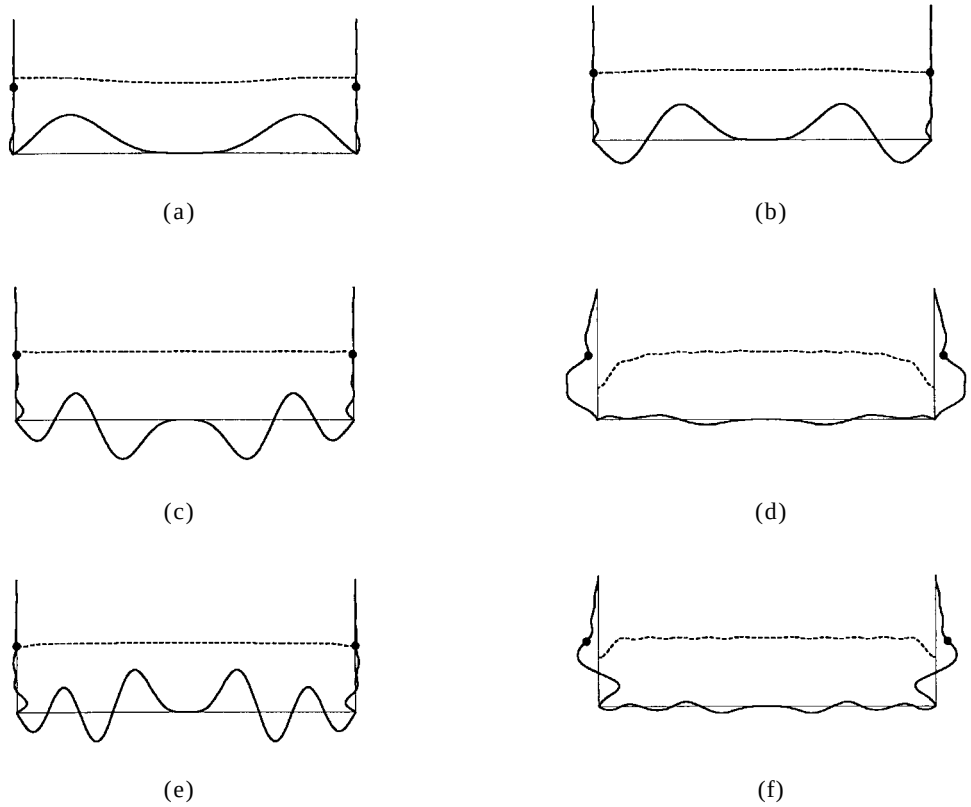

Figure 17. Mode shapes of the first six bulging modes of the studied flexible tank with a stiffener for $H = 0{\cdot}5$ m, $x^* = 0{\cdot}5$ m and $n = 4$: - - -, moving free surface; ●, location of the stiffener. (a) First P mode, frequency 19·2 Hz; (b) second P mode, frequency 45·5 Hz; (c) third P mode, frequency 83·6 Hz; (d) first S mode, frequency 88·7 Hz; (e) fourth P mode, frequency 134 Hz; (f) second S mode, frequency 168·2 Hz.

e.g. by considering either the bottom plate or the shell to be rigid. The validation, by comparing the available results in the literature, having been successfully accomplished, attention was then focused on cases where all components are flexible and free surface effects accounted for, so that the effects of various factors on the dynamics may be assessed.

The influence of the tank flexibility on the sloshing modes largely depends on the geometry of the system and the elastic properties of the tank material. However, a significant effect was observed only for very flexible tanks. More pronounced differences in sloshing frequencies of flexible and rigid tanks were observed for low liquid levels, as a consequence of the influence of the elasticity of the bottom plate.

Bulging modes are due to the elasticity of the tank, so that they are directly related to the flexibility of the shell and the base plate. It was shown that, when the shell and base plate have natural frequencies not too far from each other, global modes of the system must be studied. Storage tanks often have the bottom plate resting on a quite rigid elastic foundation, so that natural frequencies of the plate are increased. This effect was investigated also. When the base plate can be assumed rigid in the analysis, the present study has the advantage that a different rotational spring stiffness at the bottom edge of the shell can be assumed. Therefore, all the boundary conditions comprised between a simply supported and clamped bottom edge can be investigated by using the same model.

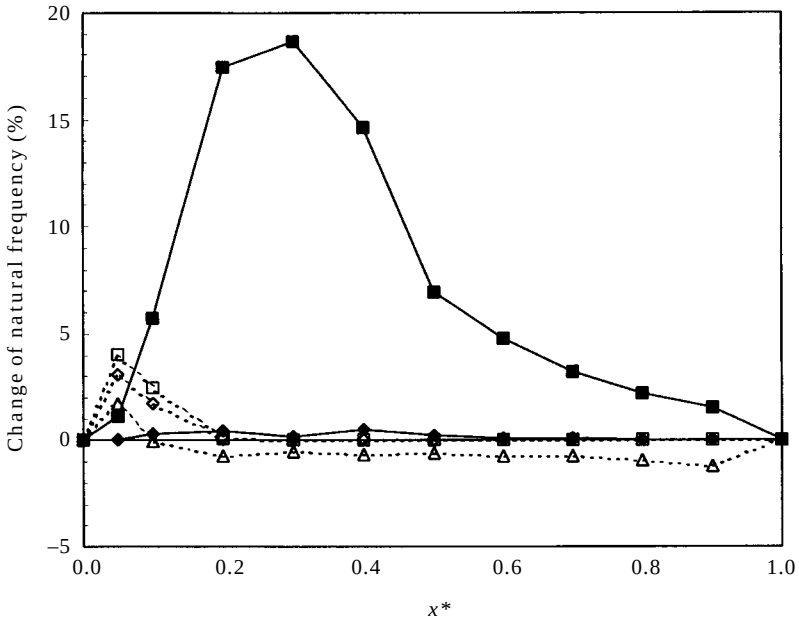

Figure 18. Percentage change of natural frequencies of the tank with one stiffener *vis à vis* the same tank without the stiffener versus the stiffener position x^*, for $H = 0{\cdot}5$ m and $n = 4$. - -□- -, First P mode; - -◇- -, second P mode; –■–, first S mode; - -△- -, third P mode; –◆–, second S mode.

Bulging modes are influenced by the free surface waves; also, in this case their effect is related to the geometry and materials of the system. Natural frequencies computed while taking into account free surface waves are higher *vis à vis* those obtained when imposing a zero dynamic pressure on the undisturbed free surface. In fact, the last condition gives a greater constraint to liquid movement, so that it overestimates the hydrodynamic mass of the system. However, for many applications the simplified free surface condition can be applied, with sufficiently accurate results.

Mode shapes of both the tank walls and free surface were shown together in order to evaluate the relative amplitudes. Interestingly, significant displacement of the free surface is also associated with bulging modes.

Ring stiffeners largely influence bulging modes of the tank; in particular, modes having a prevalent displacement of the bottom plate are greatly affected by a stiffener placed near the bottom end of the shell, while modes having a prevalent displacement of the shell are mainly affected by a stiffener placed away from the shell ends.

ACKNOWLEDGMENTS

One of the authors, Marco Amabili, gratefully acknowledges the financial support of the Research Council of Italy (CNR) for his visit to McGill University and École Polytechnique of Montreal. The authors thank a referee who kindly furnished the numerical values used in Table 7 for comparison.

REFERENCES

1. G. Bhuta and L. R. Koval 1964 *Journal of the Acoustical Society of America* **36**, 2071–2079. Hydroelastic solution of the sloshing of a liquid in a cylindrical tank.
2. H. N. Abramson (editor) 1966 *The Dynamic Behavior of Liquids in Moving Containers*, NASA SP 106. Washington, DC: Government Printing Office.
3. J. Siekmann and S. C. Chang 1968 *Ingenieur Archiv* **37**, 99–109. On the dynamics of liquids in a cylindrical tank with a flexible bottom.
4. M. Chiba 1992 *Journal of Fluids and Structures* **6**, 181–206. Nonlinear hydroelastic vibration of a cylindrical tank with an elastic bottom, containing liquid. Part I: experiment.
5. M. Chiba 1993 *Journal of Fluids and Structures* **7**, 57–73. Nonlinear hydroelastic vibration of a cylindrical tank with an elastic bottom, containing liquid. Part II: linear axisymmetric vibration analysis.
6. M. Chiba 1994 *Journal of Sound and Vibration* **169**, 387–394. Axisymmetric free hydroelastic vibration of a flexural bottom plate in a cylindrical tank supported on an elastic foundation.
7. M. Amabili 1997 *Shock and Vibration* **4**, 51–68. Bulging modes of circular bottom plates in rigid cylindrical containers filled with a liquid.
8. H. Kondo 1981 *Bulletin of the Japan Society of Mechanical Engineers* (*JSME*) **24**, 215–221. Axisymmetric vibration analysis of a circular cylindrical tank.
9. N. Yamaki, J. Tani and T. Yamaji 1984 *Journal of Sound and Vibration* **94**, 531–550. Free vibration of a clamped–clamped circular cylindrical shell partially filled with liquid.
10. R. K. Gupta and G. L. Hutchinson 1988 *Journal of Sound and Vibration* **122**, 491–506. Free vibration analysis of liquid storage tanks.
11. A. A. Lakis and M. P. Païdoussis 1971 *Journal of Sound and Vibration* **19**, 1–15. Free vibration of cylindrical shells partially filled with liquid.
12. M. A. Haroun and G. W. Housner 1982 *Journal of the Engineering Mechanics Division*, *Proceedings of the American Society of Civil Engineers* (*ASCE*) **108**, 783–800. Dynamic characteristics of liquid storage tanks.
13. M. A. Haroun and G. W. Housner 1982 *Journal of the Engineering Mechanics Division*, *Proceedings of the American Society of the Civil Engineers* (*ASCE*) **108**, 801–818. Complications in free vibration analysis of tanks.
14. P. B. Gonçalves and N. R. S. S. Ramos 1996 *Journal of Sound and Vibration* **195**, 429–444. Free vibration analysis of cylindrical tanks partially filled with liquid.
15. J. G. Berry and E. Reissner 1958 *Journal of Aeronautical Science* **25**, 288–294. The effect of an internal compressible fluid column on the breathing vibrations of a thin pressurized cylindrical shell.
16. U.S. Lindholm, D. D. Kana and H. N. Abramson 1962 *Journal of Aeronautical Science* **29**, 1052–1059. Breathing vibrations of a circular cylindrical shell with an internal liquid.
17. H. H. Bleich and M. L. Baron 1954 *ASME Journal of Applied Mechanics* **76**, 167–177. Free and forced vibrations of an infinitely long cylindrical shell in an infinite acoustic medium.
18. G. B. Warburton 1961 *Institute of Mechanical Engineers*, *Journal of Mechanical Engineering Science* **3**, 69–79. Vibration of a cylindrical shell in an acoustic medium.
19. M. K. Au-Yang 1976 *ASME Journal of Applied Mechanics* **43**, 480–484. Free vibration of fluid-filled coaxial cylindrical shells of different lengths.
20. Y. Y. Huang 1991 *Journal of Sound and Vibration* **145**, 51–60. Orthogonality of wet modes in coupled vibrations of cylindrical shells containing liquids.
21. F. Zhu 1991 *Journal of Sound and Vibration* **146**, 439–448. Orthogonality of wet modes in coupled vibration.
22. F. Zhu 1994 *Journal of Sound and Vibration* **171**, 641–649. Rayleigh quotients for coupled free vibrations.
23. F. Zhu 1995 *Journal of Sound and Vibration* **186**, 543–550. Rayleigh–Ritz method in coupled fluid–structure interacting systems and its applications.
24. H. F. Bauer 1995 *Journal of Sound and Vibration* **180**, 689–704. Coupled frequencies of a liquid in a circular cylindrical container with elastic liquid surface cover.
25. A. A. Lakis and M. Sinno 1992 *International Journal for Numerical Methods in Engineering* **33**, 235–268. Free vibrations of axisymmetric and beam-like cylindrical shells, partially filled with liquid.
26. A. Selmane and A. A. Lakis 1997 *Journal of Fluids and Structures* **11**, 111–134. Vibration analysis of anisotropic open cylindrical shells subjected to a flowing fluid.

27. M. Amabili and G. Dalpiaz 1995 *Transactions of the American Society of Mechanical Engineers, Journal of Vibration and Acoustics* **117**, 187–191. Breathing vibrations of a horizontal circular cylindrical tank shell, partially filled with liquid.
28. M. Amabili 1996 *Journal of Sound and Vibration* **191**, 757–780. Free vibration of partially filled, horizontal cylindrical shells.
29. M. Amabili, G. Frosali and M. K. Kwak 1996 *Journal of Sound and Vibration* **191**, 825–846. Free vibrations of annular plates coupled with fluids.
30. M. Amabili 1996 *Journal of Sound and Vibration* **193**, 909–925. Effect of finite fluid depth on the hydroelastic vibrations of circular and annular plates.
31. M. Amabili and M. K. Kwak 1996 *Journal of Fluids and Structures* **10**, 743–761. Free vibration of circular plates coupled with liquids: revising the Lamb problem.
32. H. F. Bauer and J. Siekmann 1971 *Ingenieur Archiv* **40**, 266–280. Dynamic interaction of a liquid with the elastic structure of a circular cylindrical container.
33. M. Amabili 1997 *Journal of Sound and Vibration* **199**, 431–452. Shell–plate interaction in the free vibrations of circular cylindrical tanks partially filled with a liquid: the artificial spring method.
34. J. Yuan and S. M. Dickinson 1992 *Journal of Sound and Vibration* **152**, 203–216. On the use of artificial springs in the study of the free vibrations of systems comprised of straight and curved beams.
35. J. Yuan and S. M. Dickinson 1992 *Journal of Sound and Vibration* **159**, 39–55. The flexural vibration of rectangular plate systems approached by using artificial springs in the Rayleigh–Ritz method.
36. J. Yuan and S. M. Dickinson 1994 *Journal of Sound and Vibration* **175**, 241–263. The free vibration of circularly cylindrical shell and plate systems.
37. L. Cheng and J. Nicolas 1992 *Journal of Sound and Vibration* **155**, 231–247. Free vibration analysis of a cylindrical shell-circular plate system with general coupling and various boundary conditions.
38. L. Cheng 1994 *Journal of Sound and Vibration* **174**, 641–654. Fluid–structural coupling of a plate-ended cylindrical shell: vibration and internal sound field.
39. L. Cheng 1996 *Shock and Vibration* **3**, 193–200. Vibroacoustic modelling of mechanically coupled structures: artificial spring technique applied to light and heavy mediums.
40. J. Missaoui, L. Cheng and M. J. Richard 1996 *Journal of Sound and Vibration* **190**, 21–40. Free and forced vibration of a cylindrical shell with a floor partition.
41. A. M. Al-Najafi and G. B. Warburton 1970 *Journal of Sound and Vibration* **13**, 9–25. Free vibration of ring-stiffened cylindrical shells.
42. A. Harari, B. Sandman and J. A. Zaldonis 1994 *Journal of the Acoustical Society of America* **95**, 3360–3368. Analytical and experimental determination of the vibration and pressure radiation from a submerged, stiffened cylindrical shell with two end plates.
43. M. Amabili 1997 *Journal of Fluids and Structures* **11**, 507–523. Ritz method and substructuring in the study of vibration with strong fluid–structure interaction.
44. D. T. Huang and W. Soedel 1993 *Journal of Sound and Vibration* **162**, 403–427. Natural frequencies and modes of a circular plate welded to a circular cylindrical shell at arbitrary axial positions.
45. L. Meirovitch 1986 *Elements of Vibration Analysis* New York: McGraw-Hill; second edition. See pp. 270–282.
46. A. W. Leissa 1973 *Vibration of Shells* NASA SP-288. Washington, DC: Government Printing Office. Now available from The Acoustical Society of America (1993).
47. A. W. Leissa 1969 *Vibration of Plates*, NASA SP-160. Washington, DC: Government Printing Office. Now available from The Acoustical Society of America (1993).
48. A. W. Leissa and Y. Narita 1980 *Journal of Sound and Vibration* **70**, 221–229. Natural frequencies of simply supported circular plates.
49. A. D. Wheelon 1968 *Tables of Summable Series and Integrals Involving Bessel Functions*. San Francisco: Holden-Day.
50. W. Soedel 1993 *Vibrations of Shells and Plates*. New York: Marcel Dekker; second edition.
51. D. J. Gunaratnam and A. P. Bhattacharya 1985 *Journal of Sound and Vibration* **102**, 431–439. Transverse vibration of circular plates having mixed elastic rotational edge restraints and subjected to in-plane forces.
52. M. Chiba 1996 *Journal of the Acoustical Society of America* **100**, 2170–2180. Free vibration of a partially liquid-filled and partially submerged, clamped–free circular cylindrical shell.
53. H. J.–P. Morand and R. Ohayon 1992 *Interactions Fluides–Structures*. Paris: Masson. See pp. 71–72. (English edition, 1995 *Fluid Structure Interaction*. New York: John Wiley.)

54. H. LAMB 1945 *Hydrodynamics*. New York: Dover. See p. 46.
55. S. WOLFRAM 1991 *Mathematica*: *A System for Doing Mathematics by Computer*. Redwood, CA: Addison Wesley; second edition.
56. M. AMABILI and G. DALPIAZ (1998) *Journal of Sound and Vibration* **210,** 329–350. Bulging modes of annular bottom plates in liquid-filled annular cylindrical tanks: theory and experiments.

APPENDIX A: SPRING MATRICES $\mathbf{K}_{P-S}$ AND $\mathbf{K}_{R-S}$

In this appendix, the partitioned spring matrix $\mathbf{K}_{P-S}$, equation (82), is given in detail. The elements of the spring submatrix $[\mathbf{K}_1]$ of dimension $N \times N$ are given by

$$[\mathbf{K}_1]_{sj} = c_1 aB^2(\pi^2/L^2)s\ j, \qquad \text{for} \quad s, j = 1, \ldots, N. \tag{A1}$$

The elements of the spring submatrix $[\mathbf{K}_2]$ of dimension $N \times (\tilde{N}+1)$ are given by

$$[\mathbf{K}_2]_{si} = -c_1 B(\pi/L)s\lambda_{ni}[A_{ni}\mathrm{J}'_n(\lambda_{ni}) + C_{ni}\mathrm{I}'_n(\lambda_{ni})],$$
$$\text{for} \quad s = 1, \ldots, N \qquad \text{and} \quad i = 0, \ldots, \tilde{N}. \tag{A2}$$

The elements of the spring submatrix $[\mathbf{K}_3]$ of dimension $(\tilde{N}+1) \times (\tilde{N}+1)$ are given by

$$[\mathbf{K}_3]_{ih} = c_1(\lambda_{ni}\lambda_{nh}/a)[A_{ni}\mathrm{J}'_n(\lambda_{ni}) + C_{ni}\mathrm{I}'_n(\lambda_{ni})][A_{nh}\mathrm{J}'_n(\lambda_{nh}) + C_{nh}\mathrm{I}'_n(\lambda_{nh})],$$
$$\text{for} \quad i, h = 0, \ldots, \tilde{N}. \tag{A3}$$

Next, the elements of the partitioned matrix $\mathbf{K}_{R-S}$, equation (84), are given by

$$\{\tilde{\mathbf{K}}_1\}_j = -k_1 aB \sin(j\pi x^*/L), \qquad \text{for} \quad j = 1, \ldots, N, \tag{A4}$$

$$[\tilde{\mathbf{K}}_2]_{sj} = k_1 aB^2 \sin(s\pi x^*/L) \sin(j\pi x^*/L), \qquad \text{for} \quad s, j = 1, \ldots, N. \tag{A5}$$

APPENDIX B: MATRIX $\mathbf{M}_L$ FOR PARTIALLY-FILLED TANKS

In this appendix the elements of the partitioned matrix $\mathbf{M}_L$, equation (97), describing the inertial effect of the liquid inside the tank, are given. The elements of the submatrix $[\mathbf{M}_1]$ of dimension $N \times N$ are given by

$$[\mathbf{M}_1]_{sj} = \rho_L aB^2 \sum_{m=1}^{\infty} \frac{4\sigma_{sm}\sigma_{jm}}{(2m-1)\pi} \frac{\mathrm{I}_n\left(\dfrac{2m-1}{2}\,\pi\,\dfrac{a}{H}\right)}{\mathrm{I}'_n\left(\dfrac{2m-1}{2}\,\pi\,\dfrac{a}{H}\right)}, \qquad \text{for} \quad s, j = 1, \ldots, N, \tag{B1}$$

where σ_{sm} are defined in equations (37a, b). The elements of the submatrix $[\mathbf{M}_2]$ of dimension $N \times (\tilde{N}+1)$ are given by

$$[\mathbf{M}_2]_{si} = \frac{1}{2}\rho_L a^2 B \left\{ \sum_{k=1}^{\infty} K_{nik}\mathrm{J}_n(\varepsilon_{nk}) \left[\zeta^{(1)}_{nsk} - \frac{\zeta^{(2)}_{nsk}}{\tanh(\varepsilon_{nk}H/a)} \right] \right.$$
$$\left. + \sum_{m=1}^{\infty} \frac{4\sigma_{sm}}{(2m-1)\pi \mathrm{I}'_n\left(\dfrac{2m-1}{2}\,\pi\,\dfrac{a}{H}\right)} (A_{ni}\xi^{(1)}_{nim} + C_{ni}\xi^{(2)}_{nim}) \right\},$$
$$\text{for} \quad s = 1, \ldots, N \qquad \text{and} \quad i = 0, \ldots, \tilde{N}, \tag{B2}$$

where K_{nik}, $\zeta^{(1)}_{nsk}$, $\zeta^{(2)}_{nsk}$, $\xi^{(1)}_{nim}$, and $\xi^{(2)}_{nim}$ are defined in equations (44), (54), (55), (59) and (60), respectively. The elements of the submatrix $[\mathbf{M}_3]$ of dimension $(\tilde{N}+1)\times(\tilde{N}+1)$ are given by

$$[\mathbf{M}_3]_{ih} = \rho_L a^3 \sum_{k=1}^{\infty} \frac{(A_{ni}\beta_{nik} + C_{ni}\gamma_{nik})}{\alpha_{nk}\varepsilon_{nk}} (A_{nh}\beta_{nhk} + C_{nh}\gamma_{nhk}) \tanh\left(\varepsilon_{nk}\frac{H}{a}\right),$$

$$\text{for} \quad i, h = 0, \ldots, \tilde{N}. \tag{B3}$$

The elements of the submatrix $[\mathbf{M}_{S1}]$ of dimension $N \times \tilde{\tilde{N}}$ are (see equation (69))

$$[\mathbf{M}_{S1}]_{sm} = \rho_L a^2 B \mathbf{J}_n(\varepsilon_{nm})\zeta^{(1)}_{nsm}, \qquad \text{for} \quad s = 1, \ldots, N \qquad \text{and} \quad m = 1, \ldots, \tilde{\tilde{N}}, \tag{B4}$$

and the elements of the submatrix $[\mathbf{M}_{S2}]$ of dimension $(\tilde{N}+1)\times\tilde{\tilde{N}}$ are (see equation (70))

$$[\mathbf{M}_{S2}]_{im} = \rho_L a^2 (A_{ni}\beta_{nim} + C_{ni}\gamma_{nim}), \qquad \text{for} \quad i = 1, \ldots, \tilde{N}+1$$
$$\text{and} \quad m = 1, \ldots, \tilde{\tilde{N}}, \tag{B5}$$

where β_{nim} and γ_{nim} are defined in equations (46) and (47), respectively.

For axisymmetric modes ($n = 0$) the submatrix $[\mathbf{M}_1]$ is unchanged; on the contrary, one has

$$[\mathbf{M}_2]_{si} = \frac{1}{2}\rho_L a^2 B \left\{ K_{0i0}\zeta^{(1)}_{0s} \sum_{k=1}^{\infty} K_{0i0}\mathbf{J}_0(\varepsilon_{0k}) \left[\zeta^{(1)}_{0sk} - \frac{\zeta^{(2)}_{0sk}}{\tanh(\varepsilon_{0k}H/a)} \right] \right.$$

$$\left. + \sum_{m=1}^{\infty} \frac{4\sigma_{sm}}{(2m-1)\pi \mathbf{I}'_0\left(\dfrac{2m-1}{2}\pi\dfrac{a}{H}\right)} (A_{0i}\xi^{(1)}_{0im} + C_{0i}\xi^{(2)}_{0im}) \right\},$$

$$\text{for} \quad s = 1, \ldots, N \qquad \text{and} \quad i = 0, \ldots, \tilde{N}, \tag{B6}$$

$$[\mathbf{M}_3]_{ih} = \rho_L a^3 \left[2\frac{H}{a}\tau_{0i}\tau_{0h} + \sum_{k=1}^{\infty} \frac{(A_{0i}\beta_{0ik} + C_{0i}\gamma_{0ik})}{\alpha_{0k}\varepsilon_{0k}} (A_{0h}\beta_{0hk} + C_{0h}\gamma_{0hk}) \tanh\left(\varepsilon_{0k}\frac{H}{a}\right) \right],$$

$$\text{for} \quad i, h = 0, \ldots, \tilde{N}. \tag{B7}$$

Moreover, for axisymmetric modes the additional column of the matrices $[\mathbf{M}_{S1}]$ and $[\mathbf{M}_{S2}]$ is

$$[\mathbf{M}_{S1}]_{s0} = \rho_L a^2 B \frac{L[1 - \cos(s\pi H/L)]}{s\pi a}, \qquad \text{for} \quad s = 1, \ldots, N, \tag{B8}$$

$$[\mathbf{M}_{S2}]_{i0} = \rho_L a^2 \tau_{0i}, \qquad \text{for} \quad i = 1, \ldots, \tilde{N}+1. \tag{B9}$$